

AD-A258 606

Elect 246

2



PL-TR-92-2100

THE MID-LATITUDE TROUGH. A REVIEW

James L. Scali

**University of Massachusetts, Lowell
Center for Atmospheric Research
450 Aiken Street
Lowell, MA 01854**

April 1992

**S DTIC ELECTE D
OCT 08 1992
A**

Scientific Report No. 2

APPROVED FOR PUBLIC RELEASE; DISTRIBUTION UNLIMITED

92-26669



**PHILLIPS LABORATORY
Directorate of Geophysics
AIR FORCE SYSTEMS COMMAND
HANSCOM AIR FORCE BASE, MA 01731-5000**

92 10 046

This technical report has been reviewed and is approved for publication.



JURGEN BUCHAU
Contract Manager



JOHN E. RASMUSSEN, Chief
Ionospheric Application Branch



WILLIAM K. VICKERY, Director
Ionospheric Effects Division

This document has been reviewed by the ESD Public Affairs Office (PA) and is releasable to the National Technical Information Service (NTIS).

Qualified requestors may obtain additional copies from the Defense Technical Information Center. All others should apply to the National Technical Information Service.

If your address has changed, or if you wish to be removed from the mailing list, or if the addressee is no longer employed by your organization, please notify PL/TSI, Hanscom AFB, MA 01731-5000. This will assist us in maintaining a current mailing list.

Do not return copies of this report unless contractual obligations or notices on a specific document requires that it be returned.

REPORT DOCUMENTATION PAGE

Form Approved
OMB No. 0704-0188

Public reporting burden for this collection of information is estimated to average 1 hour per response, including the time for reviewing instructions, searching existing data sources, gathering and maintaining the data needed, and completing and reviewing the collection of information. Send comments regarding this burden estimate or any other aspect of this collection of information, including suggestions for reducing this burden, to Washington Headquarters Services, Directorate for Information Operations and Reports, 1215 Jefferson Davis Highway, Suite 1204, Arlington, VA 22202-4302, and to the Office of Management and Budget, Paperwork Reduction Project (0704-0188), Washington, DC 20503

1. AGENCY USE ONLY (Leave blank)		2. REPORT DATE April 1992	3. REPORT TYPE AND DATES COVERED Scientific Report #2	
4. TITLE AND SUBTITLE The Mid-Latitude Trough A Review			5. FUNDING NUMBERS PE62010F PR 4643 TA 08 WUAU Contract F19628-90- K-0005	
6. AUTHOR(S) James L. Scali				
7. PERFORMING ORGANIZATION NAME(S) AND ADDRESS(ES) University of Massachusetts Lowell Center for Atmospheric Research 450 Aiken Street Lowell, MA 01854			8. PERFORMING ORGANIZATION REPORT NUMBER	
9. SPONSORING/MONITORING AGENCY NAME(S) AND ADDRESS(ES) Phillips Laboratory Hanscom AFB, MA 01731-5000 Contract Manager: Jurgen Buchau/GPIS			10. SPONSORING/MONITORING AGENCY REPORT NUMBER PL-TR-92-2100	
11. SUPPLEMENTARY NOTES				
12a. DISTRIBUTION/AVAILABILITY STATEMENT Approved for Public Release; Distribution Unlimited			12b. DISTRIBUTION CODE	
13. ABSTRACT (Maximum 200 words) The mid-latitude trough is a depletion of F-region electron densities at sub-auroral latitudes which are mostly seen as a nocturnal feature usually located between invariant latitudes 55 and 75 degrees. In this report, a review of past literature outlining the characteristics of the mid-latitude trough is presented. The material presented here will form the basis of further research in this field. In addition, procedures adopted for this research are discussed as a guide to the type of data analysis being undertaken.				
14. SUBJECT TERMS Mid-Latitude Trough, Stagnation Theory, Enhanced Recombinator, Plasma Drift, SKYMAPS, Convection Plasmopause.			15. NUMBER OF PAGES 76	
			16. PRICE CODE	
17. SECURITY CLASSIFICATION OF REPORT UNCLASSIFIED	18. SECURITY CLASSIFICATION OF THIS PAGE UNCLASSIFIED	19. SECURITY CLASSIFICATION OF ABSTRACT UNCLASSIFIED	20. LIMITATION OF ABSTRACT SAR	

TABLE OF CONTENTS

	Page
1.0 INTRODUCTION	1
2.0 CATEGORIZING TROUGHS.....	2
2.1 The High Latitude Trough.....	2
2.2 Light Ion Trough.....	7
2.3 The Daytime Trough.....	7
2.4 The Main Trough.....	11
3.0 THE PLASMAPAUSE AND THE MAIN TROUGH.....	26
3.1 The Poleward Edge of the Main Trough.....	28
4.0 MAIN TROUGH FORMATION THEORY.....	31
4.1 Stagnation Theory	31
4.2 Enhanced Recombination Theory	33
5.0 STATISTICAL STUDIES AND MODELS.....	37
5.1 Electron Temperature Enhancements in the Main- Trough Region.....	45
5.1.1 Problems Encountered with Trough Measurements.....	47
5.1.2 Physical Processes that Should be Considered for Trough Formation.....	47
6.0 USING THE AIR FORCE HIGH LATITUDE DIGISONDE NETWORK FOR TROUGH STUDIES.....	49
6.1 Data Handling Procedures.....	50
7.0 REFERENCES	62

LIST OF FIGURES

Figure No.		Page
1	Ion Spectrometer Measurements from an OGO 6 Pass on August 17, 1969. At Latitudes Poleward of -70° , Deep Localized Depressions in the O^+ and H^+ Densities Occur. This High-Latitude Trough in the Atomic Ion Density is Associated with Enhancements of the Molecular Ion Densities (Such as the NO^+ Variation Plotted). The >30 -keV Electron Trapping Boundary Location Falls Within the Trough.....	3
2	Average Locations of the High-Latitude Ionization Hole and the Main Trough Relative to a Representative Plasma Drift Configuration [After Heppner, 1977], and the Quiet Time Auroral Oval of Feldstein and Starkov [1967].	5
3	Simultaneous Measurements of Ion Composition, Electron Temperature, and Energetic Electron Flux Obtained on Four AE-C Passes Through the Winter F-Region at High Southern Latitudes.....	6
4	Relation of Morning and Afternoon Troughs to Convection.....	10
5	Schematic Diagram Depicting the Main-Trough Location, Equatorial and Poleward Edges and the Trough's Relation to the Average Position of the Plasmapause. Iso-ionic Contour Lines are Given in MHz.....	12
6	Example of Low-Altitude Trough (<1500 km) where points a and b Denote the Locations of the Top and Base of the Equatorial Edge, Respectively. Points c and d Denote the locations of the Base and Top of the Poleward Edge.....	14
7	Occurrence Frequency Distribution of Trough Minimum Position as a Function of Local Time Given in 1 Hour Intervals for 5 Seasons [from Liszka, (1967)].	16
8	A Comparison Between the Number of Troughs and K_p as a Function of Day Number Throughout May-December 1967 (Individual Points are Joined by Straight Lines for Easy Comparison of the Variation of the Number of Troughs and the K_p Index).....	18

LIST OF FIGURES (CONTINUED)

Figure No.		Page
9	The Percentage of Troughs in Each Kp Group Divided by the Percentage of Kp's in that Group for Southern Hemisphere and Northern Hemisphere.....	19
10	Trough Occurrence Frequency as a Function of Local Time for Both Hemispheres and all Longitudes from May 1967 - April 1968 [Tulunay and Sayers, (1971)]	20
11	Trough Width as a Function of Local Time Groups for Three Different Kp Groups (Trough Width Which is Defined as Being the Width Between the Two Points on each Side of the Minimum Where the Electron Density is Twice the Minimum Value).....	20
12	Trough Width as a Function of Local Time for Summer and Winter [Wildman et al., (1976)]	21
13	Diurnal and Seasonal Variation of the Equatorial Edge Trough Depth as a Function of Local Time [Wildman et al., (1976)].....	23
14	Diurnal and Seasonal Variation of the Poleward Trough Wall [Wildman et al., (1976)].....	23
15	Diurnal and Seasonal Variation of the Equatorward Trough Wall [Wildman et al., (1976)].....	24
16	Representation of Topside Ionosphere and Plasmasphere	27
17	Plasmapause and Trough at Alouette 1.....	29
18	Contours of N_mF_2 Derived from the Model of Knudsen et al., (1977). The Short-Dashed Portions of Contours are Extrapolated Contours	32

Accession For	
NTIS CRA&I	<input checked="" type="checkbox"/>
DTIC TAB	<input type="checkbox"/>
Unannounced	<input type="checkbox"/>
Justification	
By	
Distribution/	
Availability Codes	
Dist	Availability or Special
A-1	

LIST OF FIGURES (CONTINUED)

Figure No.		Page
19	(a) High-Latitude Plasma Convection Pattern Characterized by Uniform Convection Across the Polar Cap and Sunward Return Flow at Lower Latitudes. The Arrows Indicate the Direction of Plasma $E \times B/B^2$ Flow in a Reference Frame that Corotates with the Earth. (b) The Convection Pattern of Figure 19a in a Nonrotating Reference Frame. The Symmetric Form Assumed for the magnetospheric Electric Potential Distribution Leads to the Formation of a Flow Stagnation Point at 18 Hours MLT. (c) Similar to Figure 19a Except that the Convection Pattern is Modified as Discussed in the Text. (d) Result of Adding Co-Rotation to the Pattern of Figure 19a. The Flow Stagnation Point is Now Located at ~22 Hours MLT Rather Than at 18 Hours MLT as in Figure 19b.	34
20	Altitude Profiles of NO ⁺ and O ⁺ Densities for Several Effective Electric Field Strengths (mVm ⁻¹)	35
21	Trough Position, (a) Collis and Haggstrom, (b) Rycroft and Burnell	38
22	Trough Position, (a) Kohnlein and Raitt, (b) Halcrow and Nisbet.....	39
23	Trough Position, (a) Southern Edge Top, (b) Southern Edge Bottom.....	43
24	Trough Position, (a) Northern Edge Top, (b) Northern Edge Bottom.....	44
25	Structure of Electron Temperature in the Ionospheric Trough Region. The Peak of the Electron Temperature is Indicated with an Arrow. The Double Peaks of the Electron Temperature Appeared in the Magnetically Active Periods and the Distance Between Two Peaks was Large in These Periods	46
26	Linear Diurnal Variation Plots for Vz, Vh, foF2 and hmF2	51
27	Polar Plots of (a) foF2, (b) hmF2, (c) Horizontal Velocity, Vh and (d) Vertical Velocities, Vz	53

LIST OF FIGURES (CONTINUED)

Figure No.		Page
27.1	Enlarged Dusk Sector from Figure 27 Showing a Trough Detected at Goose Bay	54
28	Contour Plots for the Ratio " ρ " of Observed Quiet Day Average for the Month, March 1990 at Millstone Hill.....	56
29	Contour Plots for the Ratio " ρ " of Observed Quiet Day Average for the Month, March 1990 at Argentia.....	57
30	Contour Plots for the Ratio " ρ " of Observed Quiet Day Average for the Month, March 1990 at Goose Bay	58
31	Sequence of Ionograms Recorded at Millstone Hill When a Trough was Present.....	60
32	Sequence of Skymaps for Day 49 1990 at Millstone Hill. Each Map Combines 11 Subcases.....	61

LIST OF TABLES

Table No.		Page
1	Comparison of Previous Investigations with the Parameterized Baselevel Trough.....	15
2	Average Trough Width Values and Correlation Coefficients Between Trough Widths, Kp and Local Times.....	21
3	Summary of Features of Main Trough Types Over Halley Bay [Rodger and Pinnock, 1980].....	25

1.0 INTRODUCTION

The presence of a well defined ionization depleted sector in the F-region is known as the mid-latitude trough, often called the main trough [Muldrew, 1965; Sharp, 1966; Rodger and Pinnock, 1982]. The mid-latitude trough is generally geomagnetically oriented along a circumpolar region at an L-shell value of approximately 4. Being originally considered as the boundary region between the mid-latitude and polar ionosphere, it occurs in the northern and southern hemispheres. The most accepted view for the nature of the mid-latitude trough is that the electron densities represent the ionization level to which the entire night ionosphere would fall in the absence of external ionization sources.

One of the first observations and identification of a depletion zone in electron density measurements at F-region heights in the auroral zone was made by Muldrew [1965]. It was he who gave it the name main-trough so as to distinguish it from other temporary high-latitude troughs. However, other names have been used in the literature to describe the same ionospheric conditions. For consistency, the terms "mid-latitude" and "main" trough will be taken to mean the depletion of F-region electron densities at sub-auroral latitudes, which are mostly seen as a nocturnal feature usually between invariant latitudes 55 and 75 degrees, (or $L = 3$ to 5).

This report will review past literature on the mid-latitude trough. The characteristics of the mid-latitude trough will be discussed and suggested theories on the formation of the main trough will be outlined. The material presented here will form the basis for further research into this field. In Section 6.0 procedures adopted for this research are discussed, and some preliminary results are given as a guide to the type of data analysis being undertaken.

2.0 CATEGORIZING TROUGHS

The importance of identifying what type of trough is being observed is crucial if comparisons are to be made with previous data bases. As an example, it was pointed out by Ahmed et al. [1979], that studies of the diurnal, seasonal and altitude variations of the trough characteristics led to somewhat confusing results. Currently it has been possible to establish the presence of four types of trough. These are the main trough (or the mid-latitude trough), the high latitude trough, the light-ion trough and the daytime trough. Although as previously mentioned, attention will only be given to the phenomena producing the main trough, to complete this report, it would be best to briefly discuss these other types of trough.

2.1 The High Latitude Trough

Extensive topside ion composition measurements made aboard OGO 6 by Taylor [1972] and Taylor et al. [1975] resulted in the identification of a High Latitude Trough (H.L.T.) at $L \leq 14$ and invariant latitudes from approximately 72° to 75° . The high latitude trough is not associated with the plasmopause, but is associated with trough-like depressions in the latitudinal density distribution of atomic ions, (i.e. O^+ , H^+ etc.) while molecular ions (i.e. N_2^+ , NO^+ , O_2^+) are enhanced in the same region [Grebowsky et al., 1976]. Grebowsky et al. [1976], using ion mass spectrometer measurements from OGO 6 identified such atomic ion distributions with high latitude troughs which were often observed to lie near or on the polar cap boundary. It was concluded that the high latitude trough is not connected with the plasmopause and that soft electron flux enhancements play a role in its formation. An example of this high latitude trough is given in Figure 1, where the drop in O^+ , H^+ concentrations and an enhancement in NO^+ marks the high latitude trough region. The trough was observed to be poleward of the 70° dipole latitude in both hemispheres. The correlation between the minimum density point of the mid-latitude trough and the (> 30 keV) electron trapping boundary suggest that the origin of the H.L.T. is associated with processes which occur at or near the boundary between open and the closed magnetic field lines, and not to the localized effect of the plasmopause.

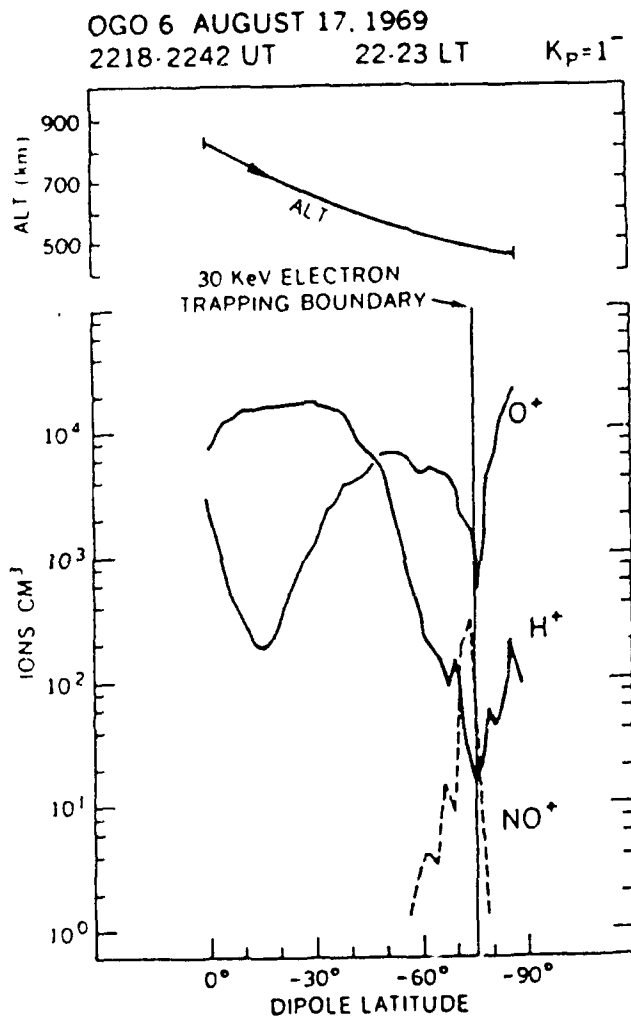


Figure 1. Ion Spectrometer Measurements from an OGO 6 Pass on August 17, 1969. At Latitudes Poleward of -70° , Deep Localized Depressions in the O^+ and H^+ Densities Occur. This High-Latitude Trough in the Atomic Ion Density is Associated with Enhancements of the Molecular Ion Densities (Such as the NO^+ Variation Plotted). The >30 -keV Electron Trapping Boundary Location Falls Within the Trough.

Further analysis using the EISCAT facility indicated that the high latitude troughs are associated with large eastward ion convection [Grebowsky et al., 1983]. These results led to the general view that increased ion recombination rates produced this depletion region. The higher recombination coefficients result from the upward moving neutral winds carrying N_2 and O_2 into the F-region due to ionospheric-magnetospheric plasma coupling during substorms.

Daytime HLT's associated with rapid westward ion drifts have also been observed [Holt et al., 1983]. Again regions of large poleward directed electric fields give rise to a rapid rate of ion-atom interchange (i.e. by the reaction $O^+ + N_2 \rightarrow NO^+ + N$) [Banks et al., 1974; Shunk et al., 1975 and Taylor et al., 1975]. The subsequent ExB ion drift leaves a trough in its wake. Similar HLT's have been reported by Evans et al. [1983] only during magnetically disturbed conditions, when these troughs move equatorwards and can be seen from Millstone Hill.

A study by Brinton et al. [1978] also identified a region where a depletion in all the measured ion densities and a minimum in Te occurred. This trough was termed the High-Latitude Ionization Hole (HLIH). Figure 2 displays this hole and its average location with respect to the auroral oval and the main trough. The ionization hole which is usually observed around 70° to 80° invariant latitude, occupies the same position as the nighttime HLT discussed above. Yet unlike the HLT the molecular ion concentrations in the HLIH also decrease. Figure 3 displays simultaneous ion composition and electron temperature for four passes of the Atmospheric Explorer (AE-C) satellite. Figure 3a which shows a path that traverses the dayside ionosphere and the auroral zone-cusp region is the only figure that shows ion molecular concentration variations consistent with the HLT as described by Grebowsky et al., 1976. The other figures clearly indicate a drop in all the atomic/molecular ion concentrations.

The results presented by Brinton et al. [1978] show that the HLIH is located poleward of the auroral zone. Also due to the nightside Te distribution being a minimum in this region, he concluded that high-speed plasma flows over the polar cap were not the cause. The dominant ion in this region was O^+ and the densities of NO^+ and O_2^+ sometimes dropped below the detection limit of approximately $3 \times 10^{+1} \text{ cm}^{-3}$. The total density in this region varied by more than a factor of 30 and sometimes reached

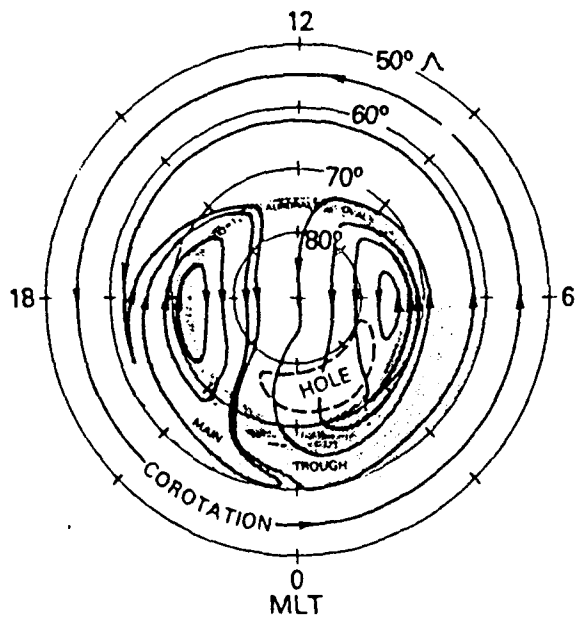


Figure 2. Average Locations of the High-Latitude Ionization Hole and the Main Trough Relative to a Representative Plasma Drift Configuration [After Heppner, 1977] and the Quiet Time Auroral Oval of Feldstein and Starkov [1967].

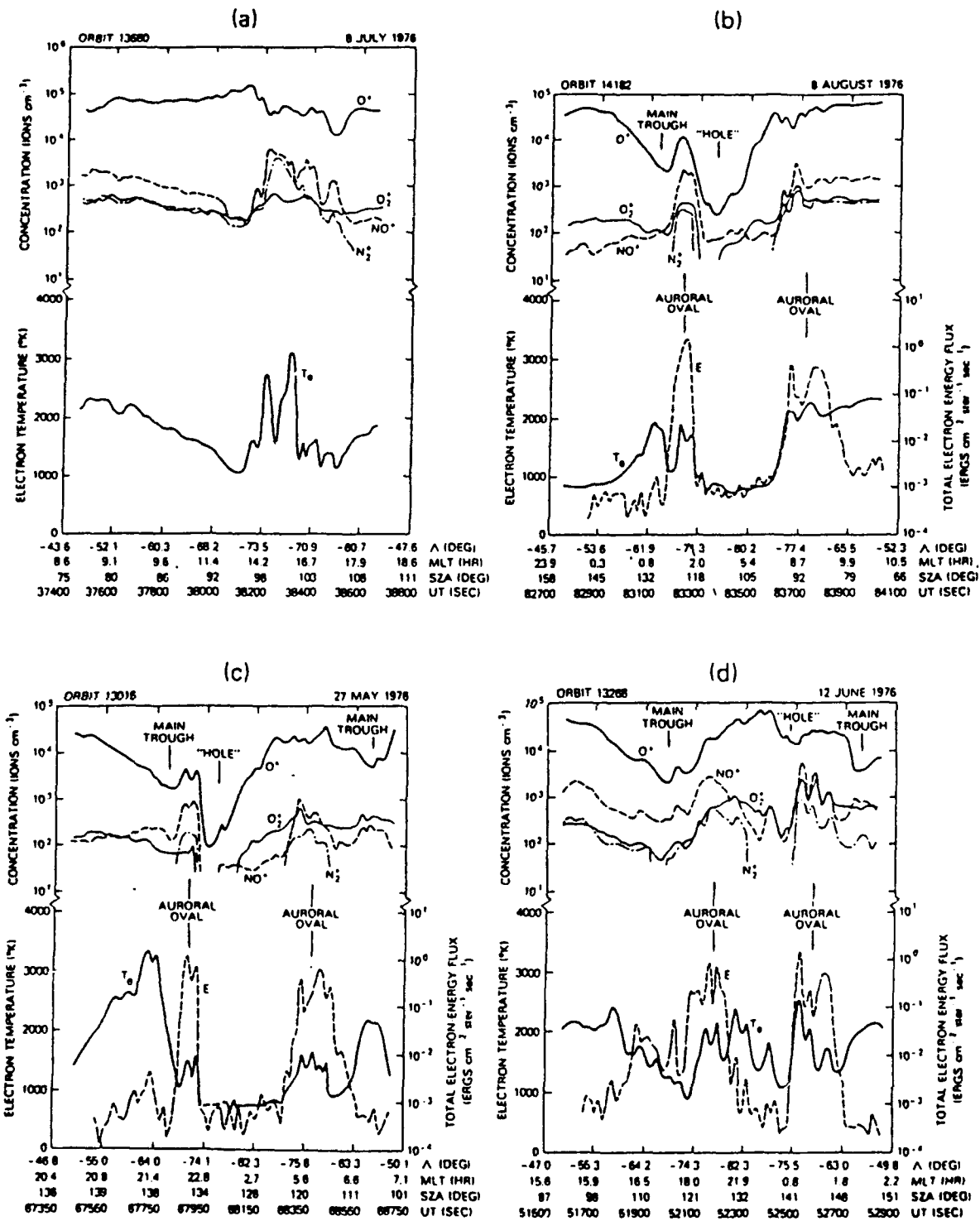


Figure 3. Simultaneous Measurements of Ion Composition, Electron Temperature, and Energetic Electron Flux Obtained on Four AE-C Passes Through the Winter F-Region at High Southern Latitudes.

values as low as $2 \times 10^{12} \text{ cm}^{-3}$, a factor of 10 below the main trough. Brinton et al. [1978] concluded that the origin of the HLIH involves very long drifts across the dark side polar cap, (particularly on the dawn side) and attendant ion recombination. On average an antisunward convection velocity of $\approx 0.1 \text{ km/s}$, corresponding to an F-region electric field convection of less than 5 mV/m , could produce the deepest trough.

2.2 Light Ion Troughs

Measurements made aboard OGO 6 by Taylor [1972] and Taylor et al. [1975], show the existence of Light Ion Troughs (LIT) at mid-latitudes ($L = 4$, $\Lambda = 60^\circ$). These light ion troughs are usually present on the dayside as well as the nightside sector [Taylor and Walsh, 1972]. The LIT is characterized by depletions of light ion (H^+ , He^+) densities, while O^+ densities remain constant in the vicinity of the plasmapause. The LIT is consistently observed, occurring 96% of the time in the nighttime hours from 1900 to 0300 LT [Ahmed et al., 1979]. A steady morning decrease in the occurrence of the LIT is observed between 0200 and 1400 LT, reaching a minimum occurrence frequency of 48% near local noon. Although Ahmed et al., 1979 used these statistics to describe the main trough, for the altitude range between 560 to 3600 km, the satellites would generally be above the heavy/light ion transition on the nightside. Hence the main trough referred to by Ahmed et al. [1979] really refers to the LIT [Moffet and Quegan, 1983].

Model calculations by Quegan et al. [1982] suggest that the LIT corresponds to the equatorward wall of the main trough for 1900 to 0600 local solar time. During the late afternoon (i.e. in the dusk sector), the LIT minimum coincides with the main trough minimum. It is observed that an increased upward H^+ flow in the daytime with increasing latitude is a major factor in producing the LIT, while at night the chemical coupling to the mid-latitude O^+ trough may be the dominant process in producing the LIT.

2.3 The Daytime Trough

Regions of depleted ionization in the daytime F-region have been known to exist for many years [Muldrew, 1965; Bowman, 1969; Tulunay and Grebowsky, 1978; Pinnock, 1985 and Whalen, 1989]. These so called daytime troughs tend to be narrower and

not as well defined as the nighttime troughs [Wildman et al., 1976]. From Ariel 4 data troughs have been observed at noon to occur at invariant latitudes of 67° to 75° [Tulunay and Grebowsky, 1978; Chacko, 1978], although troughs detected in the afternoon can be detected at $< 65^\circ$ invariant latitudes [Tulunay, 1973]. Reports on the daytime troughs at 550 km in the winter hemisphere have been shown to be dependent on both geographic and geomagnetic longitudes [Tulunay, 1973].

Daytime troughs appear to behave similar to nighttime troughs for varying levels of K_p . For instance, during very quiet magnetic activity, daytime troughs occur at high latitudes [Sojka et al., 1985]. During periods of strong magnetic activity, daytime troughs are observed at lower latitudes and are associated with large poleward directed electric fields. Evans et al. [1983] concluded that daytime troughs observed during some magnetic storms are the result of plasma sheet electrons. The redistribution of plasma in the partial ring current creates an electric field directed poleward when mapped along magnetic field lines down to the ionosphere. Further based on incoherent scatter radar observations, the features of the troughs observed by Tulunay and Grebowsky [1978] are associated with intense ion drifts [Evans et al., 1983; Holt et al., 1983]. These results being consistent with the "enhanced ion recombination" theory of Banks et al. [1974], and Schunk et al. [1975]. Observing similar westward ion drifts for daytime troughs, Spiro et al. [1978] concluded that a pre-dusk trough is formed in the nightside and that depleted plasma tubes convect westward into the afternoon sector. It was reported by Evans et al. [1983] that only during magnetically disturbed conditions and largely in winter can such daytime troughs be observed by Millstone Hill incoherent backscatter radar.

While there is at present a small amount of theoretical support to explain the formation of daytime troughs, (the general consensus being that these troughs are formed due to the effects of enhanced F2-region recombination rates along with a varying solar production term) it is clear that the formation processes of dayside F-region ionospheric troughs differ from that responsible for nighttime troughs [Pinnock, 1985]. For example Pinnock [1985] showed that:

1. Slant type sporadic E reflections are found at the trough minimum for the dayside troughs.

2. The F1-layer has a greater development when the daytime trough is present.
3. The poleward edge of the daytime trough does not have many irregularities as observed for the nighttime trough.

An excellent investigation into the daytime F-layer trough was conducted by Whalen [1987, 1989]. Using vertical incidence ionosonde data (for a large array of northern hemisphere stations) during the solar maximum period of December 1958, Whalen was able to show that daytime troughs can form either in the morning or afternoon sectors, with longitudinal extents of thousands of kilometers. Applying a simple convection cell model over the polar cap, Whalen [1989] demonstrated a pronounced longitudinal dependence of the trough which manifests itself in the afternoon sector for eastern magnetic longitudes, and in the morning sector for western magnetic longitudes. Figure 4 displays the model of the two cell convection pattern used by Whalen [1989]. The dashed circle represents the convection reversal boundary, while the shaded areas are regions where sunward convection can replace high density daytime plasma with low density nighttime plasma.

It was observed that the trough seemed to be similar to the ionospheric-magnetospheric convection pattern in morphology and activity dependence, suggesting that it results from sunward convection [Holt et. al., 1984; Foster et. al., 1985]. This requires that sunward convecting plasma displace high nighttime density plasma. Hence from Figure 4 depending on the geographic latitude of an observing ground station, it will detect an a.m. and p.m. trough. For example as the rotation of the earth carries the station at BL (Figure 4) along the path shown by the circle near 75° corrected geomagnetic latitude, its intersection with these regions correspond to its observation of the daytime troughs, i.e. the a.m. trough with the dawn cell and the p.m. trough with the dusk cell. Conversely, when the station crosses the reversal boundary on the nightside where anti-sunward convection is dominant, it will experience a relative plasma enhancement where low density nighttime plasma is displaced by higher density daytime plasma.

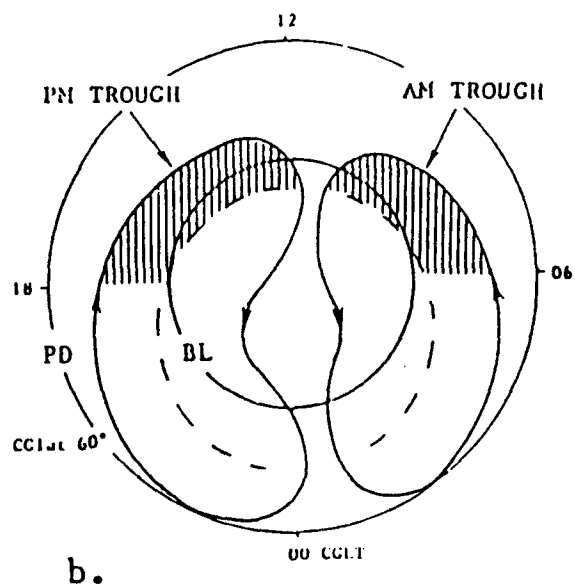
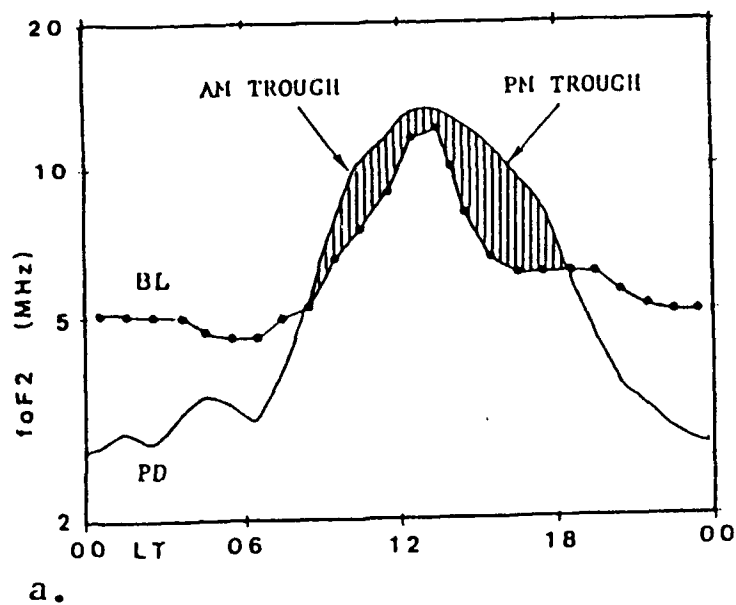


Figure 4. Relation of Morning and Afternoon Troughs to Convection.
 (a) Median foF2 from Baker Lake (BL) at 75.1° CGLat Showing AM and PM Troughs as Compared to an Undisturbed Distribution Inferred from Providenya (PD).
 (b) Schematic 2-Cell Convection Pattern Showing the AM and PM Troughs Observed in Figure a to Occur During the Passage of the Station Through Regions of the Dawn and Dusk Cells in Which High Density Daytime Plasma is Displaced by Low Density Nighttime Plasma via Sunward Convection. Conversely, BL Observes Elevated Levels at Night Which Correspond to Displacement of Nighttime Plasma by Daytime Plasma via Anti-Sunward Convection.

2.4 The Main Trough

The main trough (or the mid-latitude trough) is perhaps the most prominent feature in the nightside ion density distribution at corrected geomagnetic latitudes around 60° . Figure 5 shows a schematic diagram (obtained from Rodger and Pinnock [1982]) of the main trough location, its equatorial and poleward edges along with its relation to the average position of the plasmapause. Mostly topside sounders and some ground based measurements have been used to identify trough characteristics. These measurements establish the main trough features as:

- a) The main trough is primarily a nightside phenomenon, extending in a band from the dusk sector to the dawn sector. It is most frequently observed after ground sunset (i.e. when the solar zenith angle exceeds 90°), although it has been reported in the pre-dusk, dawn and some noon-time sectors.
- b) The main trough is more pronounced during autumn and winter months and less evident in spring and summer. In summer it is only observed near local midnight.
- c) The trough center under very quiet magnetic conditions is located near 60° corrected geomagnetic coordinates, with a width of approximately 10° at the maximum of the F-region peak [Mendillo and Chacko, 1977].
- d) The poleward edge of the trough, usually observed as a sharp increase in electron concentration, lies just equatorward of the boundary of diffuse auroral precipitation, and is usually steeper than the equatorward edge. The poleward edge generally displays a latitudinal extent of 1.5° in comparison to 7° observed for the equatorial edge.
- e) From a ground based station the latitude of the trough appears to decrease throughout the night. Since this movement is geophysical in nature, i.e. being attributed to the rotation of the earth, rather than a movement in the actual trough location, then at quiet magnetic times a movement back towards higher latitudes is observed in the dawn sector.

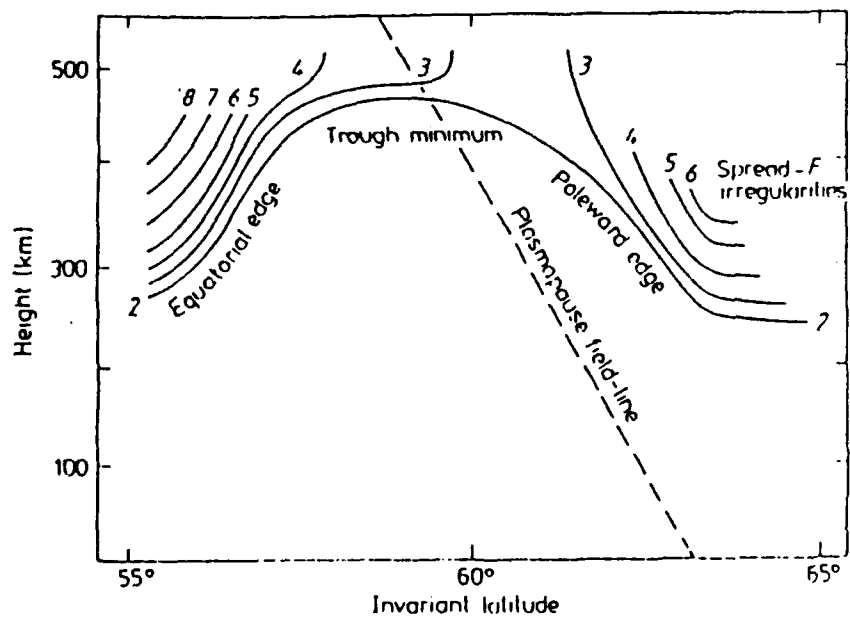


Figure 5. Schematic Diagram Depicting the Main-Trough Location, Equatorial and Poleward Edges and the Trough's Relation to the Average Position of the Plasmapause. Iso-ionic Contour Lines are Given in MHz.

- f) The position of the trough depends, among other parameters, on magnetic activity and local time. For example during periods of increased magnetic activity, the trough moves to lower latitudes.

In order for the terminology to be consistent, it is necessary to describe the main trough structure in detail. This can be done using the parameterization procedure discussed by Mendillo and Chacko [1977], and Figure 6 obtained from Ahmed et al. [1979]. The main trough then consists of the following features:

- (i) The mid-latitude gradient: is defined at lower latitudes (in this example at approximately 45 to 55 degrees invariant latitude) as the top of the equatorial edge "a".
- (ii) The equatorward trough gradient (or wall): represents the electron density drop between the top and bottom of the equatorward edge, i.e. between "a" and "b".
- (iii) The trough minimum: This value will lie between the base of the equatorial edge "b" and the base of the poleward edge "c".
- (iv) The trough poleward gradient (or wall): represents the increase in electron density between the top "d" and bottom "c" of the poleward edge.
- (v) The auroral peak: displayed by the first peak after the top of the poleward edge. The equatorward edge of the auroral oval is usually regarded as the poleward edge of the main trough [Liszka and Turunen, 1970].
- (vi) The polar gradient: usually this region is located after the auroral peak and gives an indication of the ionization concentration at higher or polar latitudes.

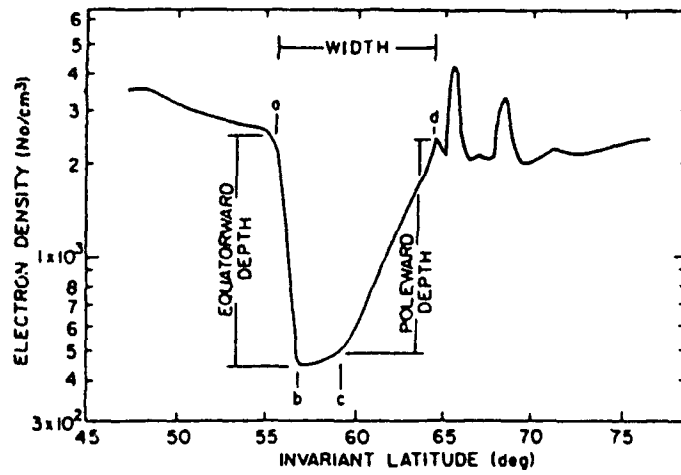


Figure 6. Example of Low-Altitude Trough (<1500 km) where points a and b Denote the Locations of the Top and Base of the Equatorial Edge, Respectively. Points c and d Denote the Locations of the Base and Top of the Poleward Edge.

From a comparison of previous investigations into the trough morphology and their parameterized base level trough, Mendillo and Chacko [1977] produced a table which lists trough positions as determined by various researchers. This table is given in Table 1. It is apparent from this table that for a mean Kp value of 0.5 we can expect the trough location to extend from approximately 48.0 to 67.5 degrees invariant latitudes at 0000 LT. In light of these observations then, features of the main trough should be observed at the ionospheric stations of Wallops Is., Millstone Hill, Argentina and Goose Bay which span invariant latitudes from 51.13° to 64.17°. It will be shown later that empirical formulas of trough position also indicate that the trough should be visible at the ionospheric stations listed.

From the analysis of 258 cases of electron content measurements made using the S-66 beacon satellite over a 15 month period (using the Faraday-rotation technique), Liszka [1967] determined seasonal and diurnal variations in the trough minimum as a function of time. Figure 7 displays the occurrence frequency distribution produced by Liszka [1967]. Due to the differing levels of magnetic activity, there is a considerable variation of trough position for all time intervals and seasons. Nevertheless an overall diurnal variation for all seasons is present.

Table 1. Comparison of Previous Investigations with the Parameterized Baselevel Trough

No.	Reference	Height	LT	\bar{K}_p	Feature	Λ , deg
<i>Ionospheric and Plasmaspheric Comparisons</i>						
1	Halcrow [1976]	h_{max}	0000	0.5	(a) top of equatorward trough wall	48.6
					(b) foot of equatorward trough wall	54.2
					(c) foot of poleward trough wall	63.8
					(d) top of poleward trough wall	66.8
2	Fenblum and Horan [1973]	h_{max}	0000	0.5	(a) top of equatorward trough wall	48.0
					(b) foot of equatorward trough wall	54.5
					(c) foot of poleward trough wall	64.5
					(d) top of poleward trough wall	67.5
3	Rycroft and Thomas [1970]	1000 km	0000	0.5	(a) center of trough	60.3
					(b) foot of poleward trough wall	64.5
					(c) top of poleward trough wall	66.1
4	Tulunay and Savers [1971]	550 km	0200-0300	<1+	center of trough	59.0
5	Chappell et al. [1970]	1400 km*	0200	0.5	H* plasmopause position	63.2
6	H A Taylor et al [1969]	1400 km†	near 0000	0.5	H* plasmopause position	65.3
<i>Comparisons With Related Phenomena</i>						
7	Aarons and Allen [1971]	350 km	0000	0.5	average location of F region irregularity boundary determined by scintillation measurements	≈61.5
8	Sheehan and Carovillano [1976]		0000	0.5	equatorward edge of aurora for November-December	≈67
9	Lui et al [1975]		0000	0.5	equatorward edge of the diffuse aurora	≈67
10	Feldstein [1966]		0000	0.5	midpoint of the 0000 LT segment of the auroral oval	≈70

*L = 6 measured near the equatorial plane corresponds to $\Lambda = 63.2^\circ$ at 1400 km.

†L = 7 measured near the equatorial plane corresponds to $\Lambda = 65.3^\circ$ at 1400 km.

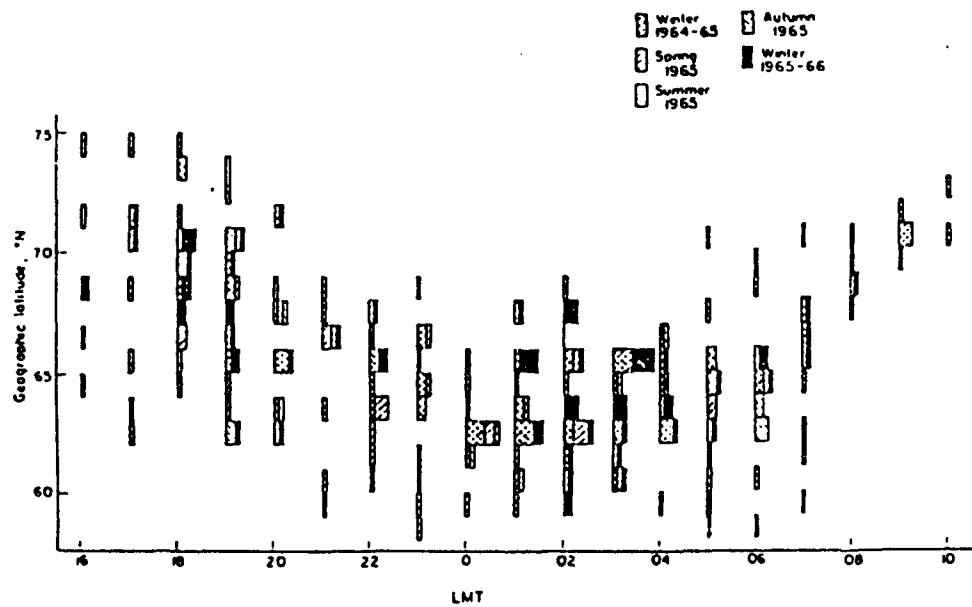


Figure 7. Occurrence Frequency Distribution of Trough Minimum Position as a Function of Local Time Given in 1 Hour Intervals for 5 Seasons [from Liszka, (1967)].

Using electron density data collected from the experiment aboard the Ariel III satellite, Tulunay and Sayers [1971] were able to identify 1287 troughs in both the southern and northern hemispheres. It was shown that 84% of the computer selected troughs could be considered as mid-latitude troughs as described by Muldrew [1965]. The results presented by Tulunay and Sayers [1971] indicated:

- (i) that there is a preference for geomagnetic alignment of troughs rather than geographic,
- (ii) from their Figure 2a (reproduced here as Figure 8), it was immediately obvious that the occurrence of troughs varies in a similar manner to the magnetic activity in that higher Kp is associated with a greater number of detected troughs. Further analysis (Figure 9) confirmed that more troughs are produced when Kp is high.
- (iii) taking into account both hemispheres it was shown (Figure 10) that during the period of May 1967 to April 1968, troughs tend to be detected more frequently around 0300 to 0400 LT. A second smaller peak at 1800 LT is also observed.
- (iv) defining the "trough width" as the width between the two points on each side of the minimum where the electron density is twice the minimum value, Tulunay and Sayers [1971] observed that as Kp increases the widths of the troughs begin to decrease (Figure 11). From Figure 11 it is apparent that the trough width is greatest during the early morning and late evening. Unfortunately no indication of the vertical scale was given. However, a feeling for the scale of these widths is given in Table 2, which gives typical values of correlation coefficients between the trough widths, Kp and LT as well as average trough width values.

An analysis of the trough width was conducted by Wildman et. al., [1976]. Their results were based on 1000 individual trough measurements made by the INJUN5 and ISIS1 satellite, which measured the in situ positive ion and electron concentrations respectively. Figure 12 shows some results from this analysis. A simple diurnal variation is observed which has a maximum at approximately 0300

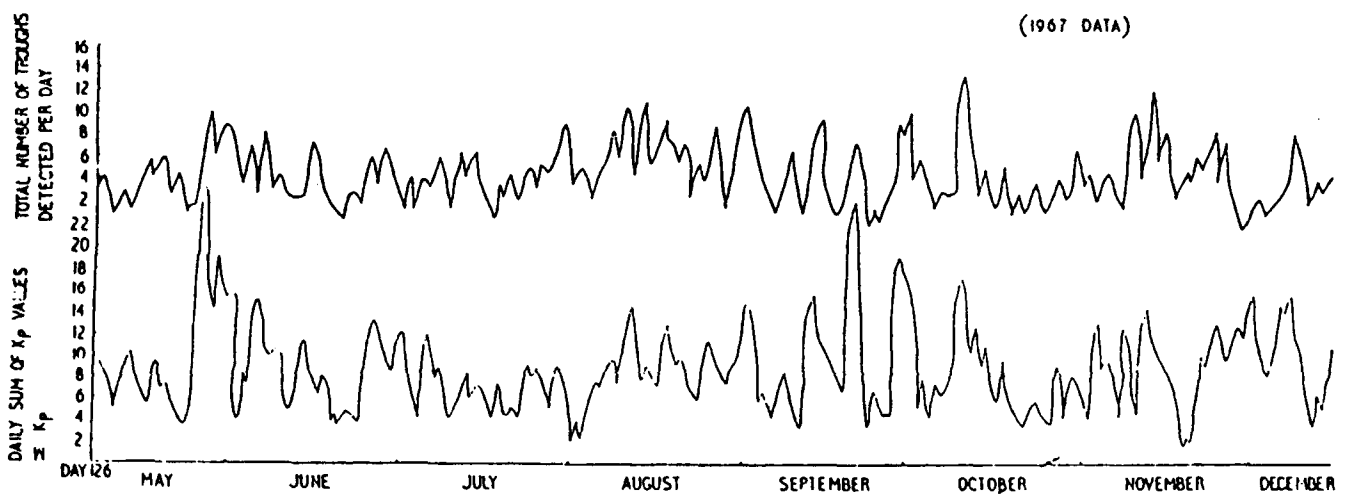


Figure 8. A Comparison Between the Number of Troughs and K_p as a Function of Day Number Throughout May-December 1967 (Individual Points are Joined by Straight Lines for Easy Comparison of the Variation of the Number of Troughs and the K_p Index).

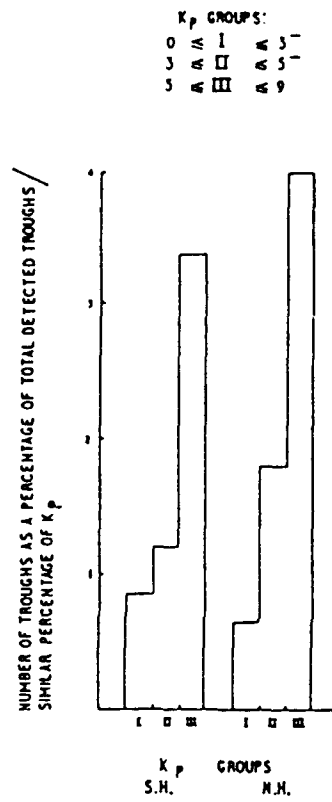


Figure 9. The Percentage of Troughs in Each K_p Group Divided by the Percentage of K_p's in that Group for Southern Hemisphere and Northern Hemisphere.

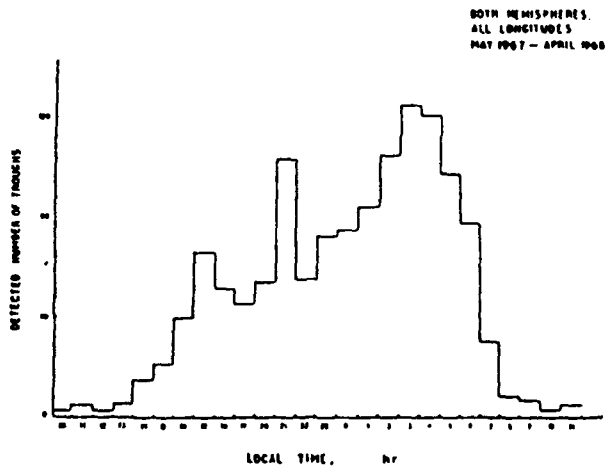


Figure 10. Trough Occurrence Frequency as a Function of Local Time for Both Hemispheres and all Longitudes from May 1967 - April 1968 [Tulunay and Sayers, (1971)].

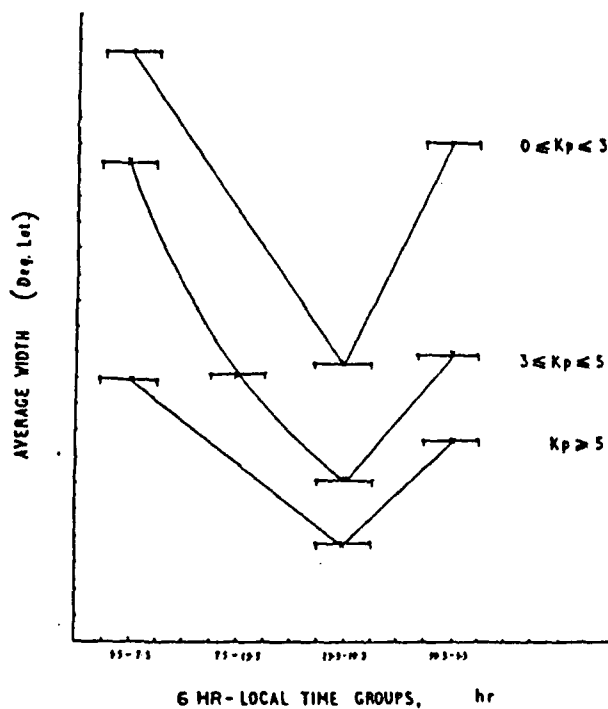


Figure 11. Trough Width as a Function of Local Time Groups for Three Different Kp Groups (Trough Width Which is Defined as Being the Width Between the Two Points on each Side of the Minimum Where the Electron Density is Twice the Minimum Value).

Table 2. Average Trough Width Values and Correlation Coefficients Between Trough Widths, K_p and Local Times

Northern hemisphere summer: Sample size: 19, All K_p , LT: 1 00-2 00	
Average width \pm standard deviation	13.56 \pm 8.81
R_{12} = Linear correlation coef. between width and K_p , ignoring LT	-0.663
$R_{m,12}$ = Linear multiple correlation coef. of width on K_p and LT	0.667
$R_{p,12}$ = Linear partial correlation coef. between width and K_p , keeping LT constant	-0.513
Northern hemisphere winter: Sample size: 25, $K_p < 3$, LT: 6 00-7 00	
Average width \pm standard deviation	10.98 \pm 3.81
R_{12}	-0.367
$R_{m,12}$	0.420
$R_{p,12}$	-0.347
LT: 22 00-2 00 Sample size: 13, $K_p < 3$	
Average width \pm standard deviation	10.56 \pm 5.63
R_{12}	-0.843
$R_{m,12}$	0.236
$R_{p,12}$	-0.826

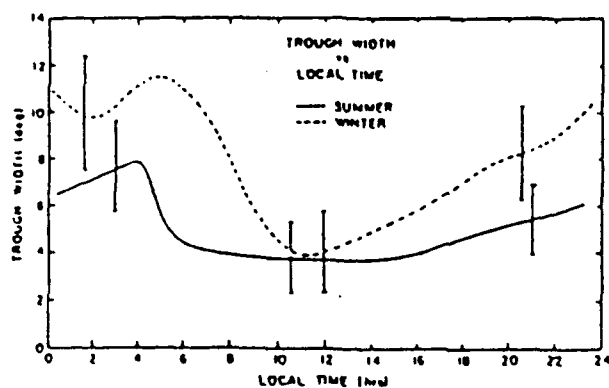


Figure 12. Trough Width as a Function of Local Time for Summer and Winter [Wildman et al., (1976)].

to 0500 LT, and a minimum of about 4 degrees around noon. This is a constant feature throughout all seasons although the greatest variability in the width of the trough is seen in winter. The trough width was typically observed to be around 7 to 10 degrees [Evans et al., 1983].

Another feature observed was the variation of trough depth with local time. Observations by Wagner et al., [1973] revealed a minimum in the main trough density in the early morning hours. However, Brinton et al. [1978] observed that the trough is deepest near dusk (i.e. 1900 MLT). Brinton et al. [1978] also states that a hemispheric difference is observed in the variation of the main trough depth with local time. For the time intervals studied, the trough densities measured in the northern hemisphere were lowest in the postmidnight sector. Although this behavior may not reflect true hemispheric asymmetry, since in the need to make measurements at high magnetic latitudes, AE-C operations were usually scheduled for western longitudes in the northern hemispheres and eastern longitudes in the southern hemispheres. The differences in longitudes and seasons were not taken into account.

Defining the trough depth as the ratio of plasma density at the leading trough edge to the plasma density value at the base of the trough wall, Wildman et al., [1976] also analyzed this feature. Figure 13 displays the results of the diurnal and seasonal variations of the equatorial edge of the trough depth. The trough depth is maximum around midnight, with a minimum value around noon. The diurnal variation in the trough depth during summer varies by as much as 67% and by 90% during winter. This difference in seasons results from the reduction in the solar radiation contribution to ionization in the polar regions in winter.

Wildman et al. [1976] also discussed the trough gradients, in particular the poleward and equatorward edges. Figures 14 and 15 display the diurnal and seasonal behavior of the poleward and equatorward trough wall gradient for each season respectively. In general all summer gradients are very much reduced when compared to winter gradients, except near 1100 LT. The largest gradients are observed during equinoxes, but interestingly enough, while large gradients are observed around midnight for

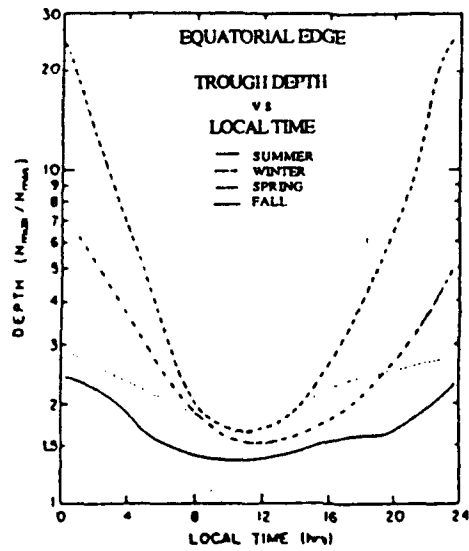


Figure 13. Diurnal and Seasonal Variation of the Equatorial Edge Trough Depth as a Function of Local Time [Wildman et al., (1976)].

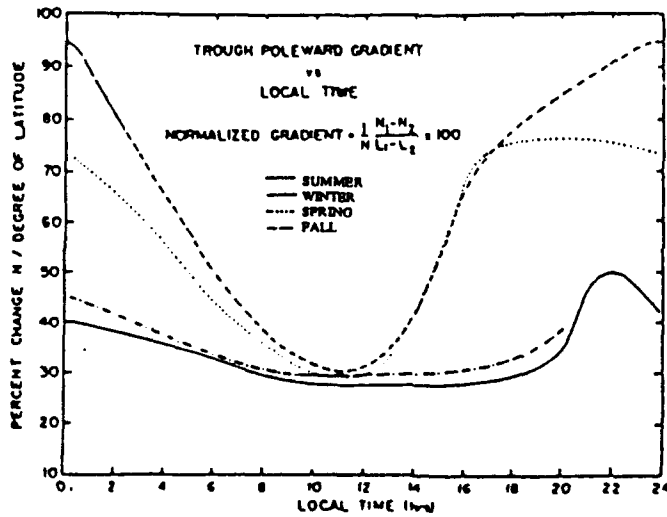


Figure 14. Diurnal and Seasonal Variation of the Poleward Trough Wall [Wildman et al., (1976)].

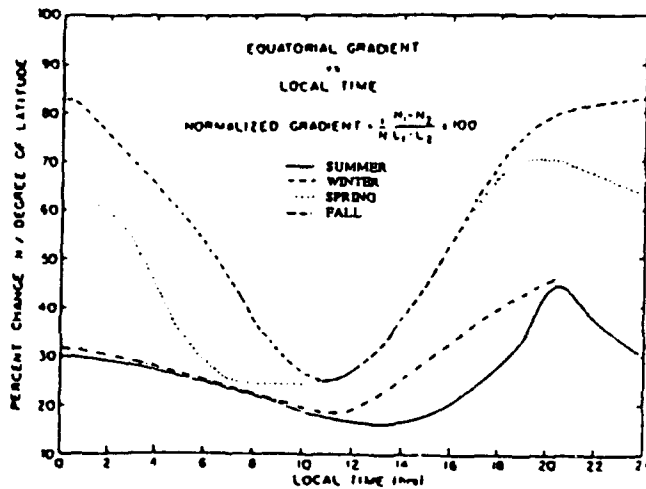


Figure 15. Diurnal and Seasonal Variation of the Equatorward Trough Wall [Wildman et al., (1976)].

both poleward and equatorward edges, the gradients are greatly reduced around 1100 LT. At this time gradient values correspond closely to those observed during solstice. This suggests that the morphology of daytime troughs (at least around 1100 LT) are the same for all seasons.

As mentioned previously, the main trough moves to lower latitudes when magnetic activity increases. From early results Sharp [1966] for a short sample of observations did not notice any change in the geomagnetic location of the mid-latitude trough. Muldrew [1965] on the other hand, drawing from results taken over a period of several months, noticed that the geomagnetic location of the trough did change and seemed to be greatly influenced by magnetic activity. Rodger and Pinnock [1982] further discussed the movement of the trough over Halley Bay (Antarctica). They observed rapid movement across the station in the early hours of the night, and a decreased speed later in the night. They interpreted this movement as the trough being stationary in UT and the movement therefore being due to the rotation of the earth. However, as they pointed out the trough will move equatorwards during geomagnetically disturbed times. Rodger and Pinnock [1980] further classified the main troughs observed into five types, dependent on Kp, time of occurrence, sporadic-E and spread-F. A listing of these types are given in Table 3.

Table 3. Summary of Features of Main Trough Types Over Halley Bay
[Rodger and Pinnock, 1980].

	Type 1	Type 2	Type 3	Type 4	Type 5
Time of occurrence (local zone time)	1600-2000	2000-2300	2300-0100	0100-0500	usually after 0100
Magnetic activity (K_p)	≥ 5	3-5	3-5	2	< 2
Time to cross Halley Bay (h)	2	3	3	4	Does not cross
Storm types of sporadic E	Always	Usually	Seldom	None	None
Conditions following trough	Blackout; high latitude ridges very disturbed	Similar type to 1 but less severe	Very extensive spread - F blackout rare	Extensive spread - F	Sunrise ends sequence

Muldrew [1965] and Grebowsky et al. [1978] also stated that the trough position could be better correlated by noting that an increase in K_p corresponds to a decrease in trough latitude position with a lag time of 5 to 17 hours. This is in general agreement with the findings of Feinblum et al [1968] who concluded that foF2 was better correlated with K_p observed twelve hours earlier.

The association of sporadic E and spread F with the main trough has also been investigated [Nichol, 1973; Rodger et al, 1983]. The occurrence of sporadic E (Es) under the main trough region observed from Halley Bay, Antarctica, revealed that two types of Es occurred [Morrell, 1983]. The first type occurs before magnetic midnight and exhibits a semi-thickness similar to the normal daytime E-layer, while the second type occurring after midnight is much thinner. It was suggested that the source of the pre-midnight electron precipitation contributes to the ionization level. However, since no mention of the effects of neutral winds was made, the study made by Morell [1983] is incomplete in terms of describing the processes that cause the Es layer observed with the main trough.

3.0 THE PLASMAPAUSE AND THE MAIN TROUGH

Figure 16 displays a simplified view of the topside ionosphere and plasmasphere. This figure serves as a good basis in understanding the approximate locations of the troughs, auroral zone and plasmasphere. The plasmopause was first defined by Carpenter [1966] as an abrupt change in the charged particle concentration in the atmosphere. Rycroft [1975] gave two definitions of the plasmopause, these are:

- (i) Ionospheric Plasmopause: The ionospheric plasmopause is the ionospheric surface separating plasma that co-rotates with the earth and plasma that precipitates from magnetospheric convection processes.
- (ii) Equatorial Plasmopause: This is Carpenter's [1966] definition and states that the plasmopause is the region where an order of magnitude or more decrease in electron density with increasing radial distance, within a fraction of an earth radius R_e in the equatorial plane is detected.

Moffet and Quegan [1983] and Grebowsky et al. [1974] hold the view that a distinction should be made between an ionospheric (or convection) plasmopause and an equatorial plasmopause, since the ionospheric plasmopause is related to convection processes and will be better correlated with the movement of the trough during magnetically disturbed times. Chappell [1972] discusses how the plasmopause shrinks in the equatorial plane with increasing magnetic activity. This process induces large westward plasma drifts in the ionosphere around 1400-1800 LT [Evans, 1975; Mendillo and Klobucher, 1975]. Through ion-recombination this process will cause an electron depletion in the F-region equatorwards of the plasmopause [Tulunay and Sayers, 1971; Halcrow, 1976]. Kavanagh et al. [1968] was able to show that following a magnetic storm the plasmasphere shrinks in size and is accompanied by a marked earthward movement, while at the same time the trough moves equatorward.

Originally it was thought that the main trough marked the boundary between the solar controlled mid-latitude ionosphere and the auroral ionosphere, which is chiefly controlled by plasma convection and plasma particle precipitation processes. It was not clear whether the foot of the magnetic field line marking the plasmopause

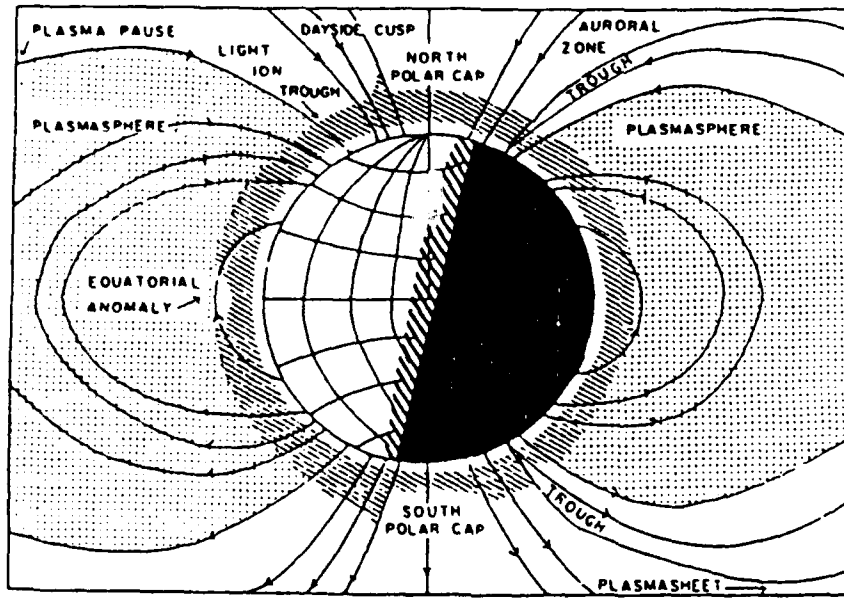


Figure 16. Representation of Topside Ionosphere and Plasmasphere

fell along the equatorial edge of the trough or its center. Rycroft and Thomas [1970], from a statistical study of the position of the main trough and plasmopause at 1000 km altitude, showed that the center of the plasmopause and trough minimum lie on the same geomagnetic line of force, (typically at $L = 4$ or $\Lambda = 57^\circ$). Figure 17 reproduced from this paper illustrates this result clearly. While Grebowsky et. al., [1976a] using individual cases did not come to the same conclusion, it is generally accepted that the equatorial plasmopause and the main trough minimum occur on nearly the same L-shell but that the equatorial plasmopause can be observed just equatorward of the main trough minimum for most of the night. However, under steady geomagnetic conditions, in the morning hours, the poleward edge of the trough and the plasmopause are thought to be closely related [Quegan et al., 1982; Rodger and Pinnock, 1982]. Usually the equatorial plasmopause and the ionospheric plasmopause do not coincide. So it is uncertain how the ionospheric plasmopause relates to the main trough minimum position.

Rycroft and Thomas [1970] derived an empirical relation for the equatorial radial distance R_p (measured in R_e) to the center of the plasmopause for local midnight. This was given as:

$$R_p = 5.64 - (0.78 \pm 0.12) K_p^{0.5}$$

Other empirical relations for the mid-latitude plasmopause location are given as:

$$\begin{array}{ll} \Lambda_p = 4.65 - 0.23 K_p & \text{Brace and Theis [1974]} \\ \Lambda_p = 5.70 - 0.47 K_p & \text{Carpenter and Park [1973]} \end{array}$$

where Λ_p = the invariant latitude of the plasmopause in degrees and $K_p > 3$

3.1 The Poleward Edge of the Main Trough

Data from both the dynamics explorer.2 (DE-2) and the advanced ionospheric sounder (AIS) at Halley (Antarctica) were used by Rodger et al. [1986] to analyze the formation, orientation and dynamics of the poleward edge of the main trough. From these investigations Rodger et al. [1986] concluded that:

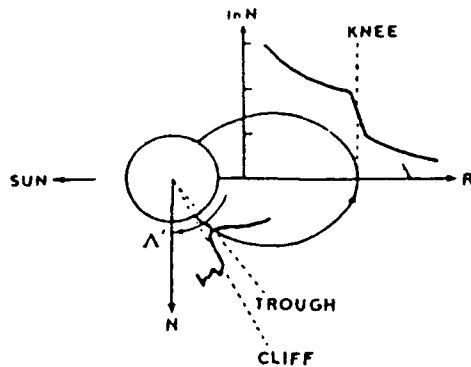


DIAGRAM ILLUSTRATING THE RESULT THAT A PARTICULAR LINE OF FORCE OF THE GEOMAGNETIC FIELD ($L \sim 4$) PASSES THROUGH BOTH THE MINIMUM OF THE ELECTRON DENSITY TROUGH AT THE ALOUETTE I ORBIT AND THE CENTRE OF THE MAGNETOSPHERIC PLASMAPAUSE.

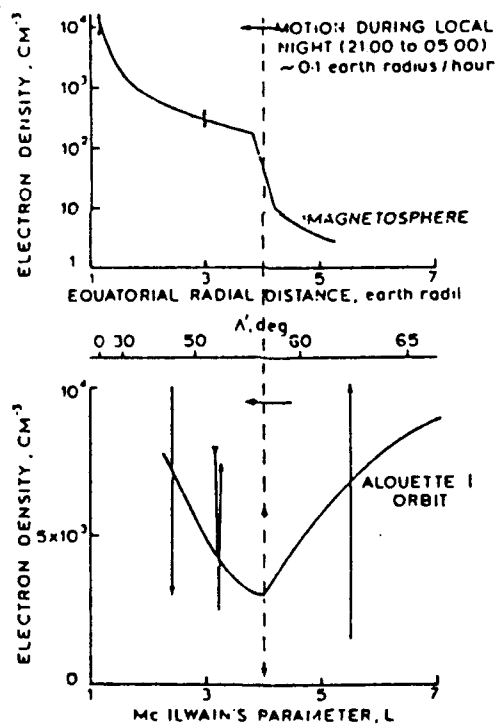


DIAGRAM ILLUSTRATING THE RESULT THAT THE CENTRES OF THE PLASMAPAUSE AND TROUGH LIE ON THE SAME GEOMAGNETIC LINE OF FORCE. TYPICALLY $L \sim 4$, OR $\lambda' \sim 57^\circ$, FOR $K_p \sim 3$ AT 02.00 LT. Typical magnetospheric and ionospheric profiles are shown, together with their behaviour with changing local time.

Figure 17. Plasmapause and Trough at Alouette 1

- (a) Before magnetic midnight, local particle precipitation appears to be mainly responsible for the formation of the poleward edge of the main trough for all seasons.
- (b) Convection of plasma, perhaps from the polar cusp, appears to be the most important process in forming the poleward edge of the trough after magnetic midnight when geomagnetic activity is steady or decreasing. But when magnetic activity is increasing then local particle precipitation may be important. A more quantitative analysis is required to determine the relative importance of the various sources of plasma which form the poleward edge of the trough in the morning sector.
- (c) There is often a significant increase in the flux of the conjugate photo-electrons coincident with the poleward edge of the trough in the morning sector. Although a few possible explanations have been discussed no firm conclusion has been made.
- (d) The region immediately equatorward of the poleward edge of the trough has very high electron temperatures [Brace et al., 1982]. This may be due to the heating associated with stable auroral arcs [Nagy et al., 1970; Craven et al., 1982], and may effectively reduce the inter-hemispheric flow of photo-electrons. Since the coulomb collision rate is affected by the electron temperature then the flow of photo-electrons from the conjugate hemisphere in the trough minimum region may be reduced.
- (e) The orientation of the poleward wall changes appreciably as a function of LT. Also the latitudinal dynamics can be very different on nights when similar geomagnetic conditions prevail.

4.0 MAIN TROUGH FORMATION THEORY

In discussing the formation of the main-trough one needs to consider processes such as plasma convection, ion chemistry, plasma escape and neutral winds. It appears that no one process is totally consistent with day or nighttime observed troughs. Indeed given the observational evidence available a number of theories give alternative explanations of certain types of troughs (Rodger et al., 1992). Among these theories Schunk et al. [1976] discussed the possibility that an upward flow of H^+ in the polar wind along the magnetic field lines can decrease O^+ levels which in turn contribute to the rate of decay of the F-layer. Yet this process alone cannot account for the total ionization depressions observed in the trough. Murphy et al. [1976] suggested that F-layer electron density levels could be further depressed by up to 15% by the replenishment of the protonosphere after a magnetic storm.

Enhanced molecular nitrogen concentrations during periods of high magnetic activity in the sub-auroral zone were also considered as contributing to trough formation [Raitt et al., 1975; Prolss and Von Zahn, 1974]. But again this process is insufficient to explain the size of the troughs reported [Wrenn and Raitt, 1975; Schunk et al., 1976]. The two most promising theories to explain the formation of the nocturnal trough are the so called stagnation and enhanced recombination theories. It is these two theories that will be discussed in the following sections.

4.1 Stagnation Theory.

First proposed by Knudsen [1974], the stagnation theory takes into account the competing effects of the rotation of the earth and the auroral electric field induced convection [Knudsen et al., 1977; Spiro et al., 1978]. The theory states that flux tubes containing F-region plasma are convected from day to night across the polar cap, (with speeds typically of the order of 0.5 - 1.0 km/s). This plasma motion directed in an antisunward direction would form a tongue of ionization across the polar cap as shown in Figure 18 (taken from Knudsen et. al., [1977]). Upon reaching the nightside the flux tubes containing F-region plasma return to the dayside by drifting through the dawn and dusk sectors at low latitudes. The competing effects of this two-cell plasma flow (one directed eastward and the other directed westwards shown in Figure 18) and the earth's rotation would result in the formation of a trough around 1800 magnetic local time.

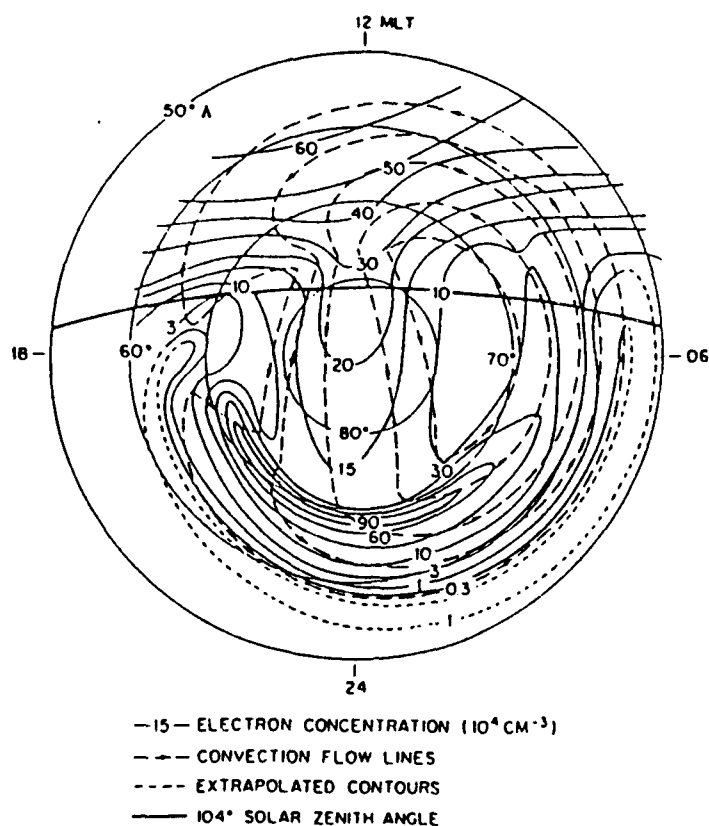


Figure 18. Contours of $N_m F_2$ Derived from the Model of Knudsen et al., (1977).
The Short-Dashed Portions of Contours are Extrapolated Contours.

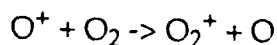
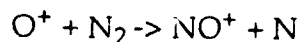
As an example, those flux tubes that return via the dusk sector must drift faster than the rotation of the earth if they are to reenter the dayside. The effect tends to confine the same flux tubes to a "stagnation" region in the evening sector for longer periods of time. Then the loss of ionization in these flux tubes by recombination is thought to lead to the formation of a trough. This trough would then drift from the dusk through midnight towards the dawn sector. It is believed that the trough forms primarily from the increased time available for ionization to decay via normal recombination processes within these flux tubes, and not from any external enhanced recombination [Kundsen, 1974; Kundsen et al., 1977 and Spiro et al., 1978]. Although the process is further complicated by the separation of the geographic and geomagnetic poles (which define the solar terminator and the location of the auroral electric field convection patterns respectively), detailed calculations made by Sojka et al. [1981a, b] show that the stagnation theory does work.

Spiro et al. [1978] used AE-C data to examine the actual plasma flow patterns and then further redefined the stagnation mechanism. The basic convection pattern presented by Knudsen [1974] was modified such that the position of the stagnation point changed as many new features observed by the satellite were included. These results are supplied in Figure 19. Figures 19a and b represent the simple configuration suggested by Knudsen [1974]. In Figure 19c the basic convection pattern is offset by some 5° towards the nightside sector to reflect the day/night asymmetry. In Figure 19d corotation is added to this pattern and alters the field flow. The result is that the stagnation region is shifted from 1800 MLT to about 2200 MLT.

A drawback of the stagnation theory is that it requires the convection pattern to be consistent long enough for recombination of ionization to form the trough. However, if expansion/contraction of the auroral oval due to substorms were to occur, then it is unclear as to whether a trough can still develop due to this mechanism [Evans et al., 1983].

4.2 Enhanced Recombination Theory

Under the influence of large electric fields, enhanced ionic recombination in the polar cap plasma convection pattern can be shown to contribute to the formation of a main trough. In particular the increase in electric fields lead to an increased rate of loss of O⁺ in the reactions with N₂ and O₂ given as:



Banks et al. [1974] and Schunk et al. [1975] showed that ion drifts induced by electric fields act in two ways to increase the reaction rates of the reactions above: 1. as a result of Joule heating the ion temperature increases and 2. through the dependence of the reactions upon the relative flow speeds of the ion and neutral gases. Figure 20 (taken from Schunk et. al., [1975]) displays the altitude profiles of O⁺ and NO⁺ for several electric field strengths. The decrease in O⁺ concentration is quite clear with increasing electric field values, and while for altitudes around 200 km NO⁺ does not seem to vary greatly, at higher altitudes an increase in NO⁺ concentrations with increasing electric fields is apparent.

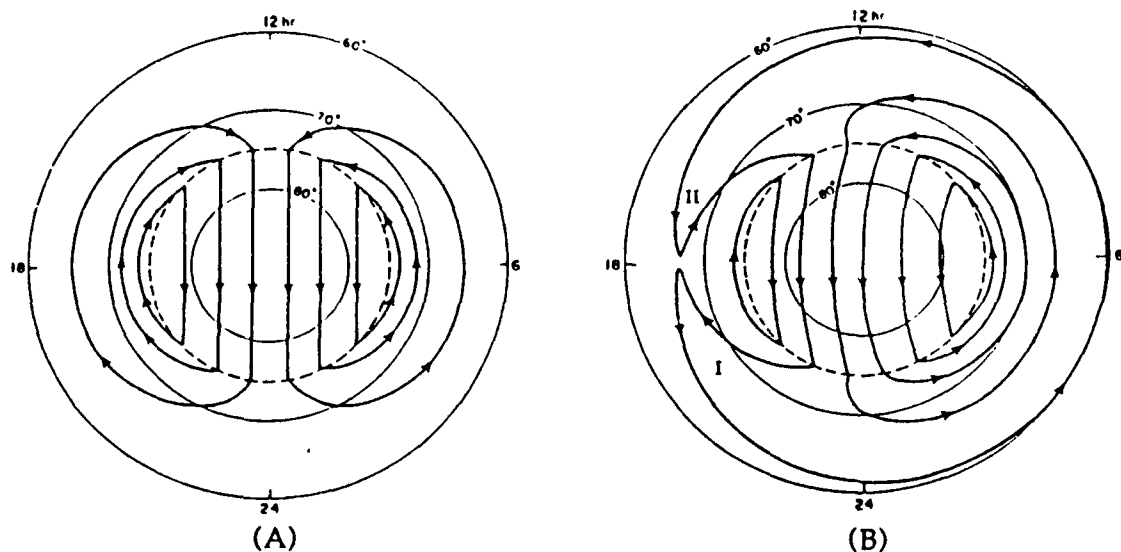


Figure 19. (a) High-Latitude Plasma Convection Pattern Characterized by Uniform Convection Across the Polar Cap and Sunward Return Flow at Lower Latitudes. The Arrows Indicate the Direction of Plasma $E \times B/B^2$ Flow in a Reference Frame that Corotates with the Earth.

(b) The Convection Patter of Figure 19a in a Nonrotating Reference Frame. The Symmetric Form Assumed for the magnetospheric Electric Potential Distribution Leads to the Formation of a Flow Stagnation Point at 18 Hours MLT.

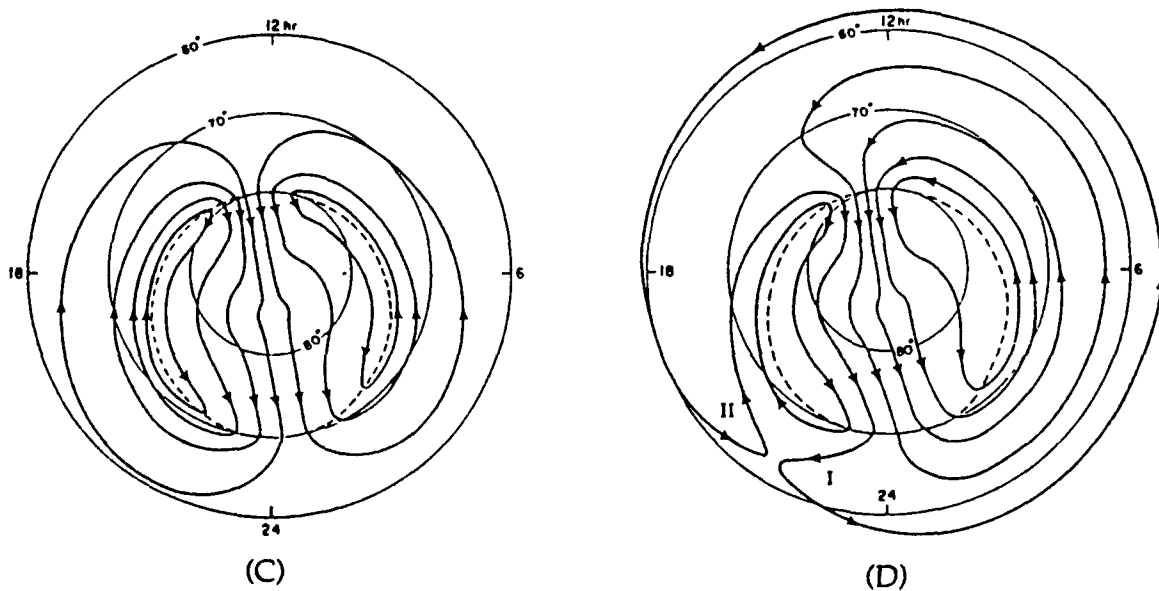


Figure 19 (c) Similar to Figure 19a Except that the Convection Pattern is Modified as Discussed in the Text.

(d) Result of Adding Co-Rotation to the Pattern of Figure 19a. The Flow Stagnation Point is Now Located at ~22 Hours MLT Rather Than at 18 Hours MLT as in Figure 19b.

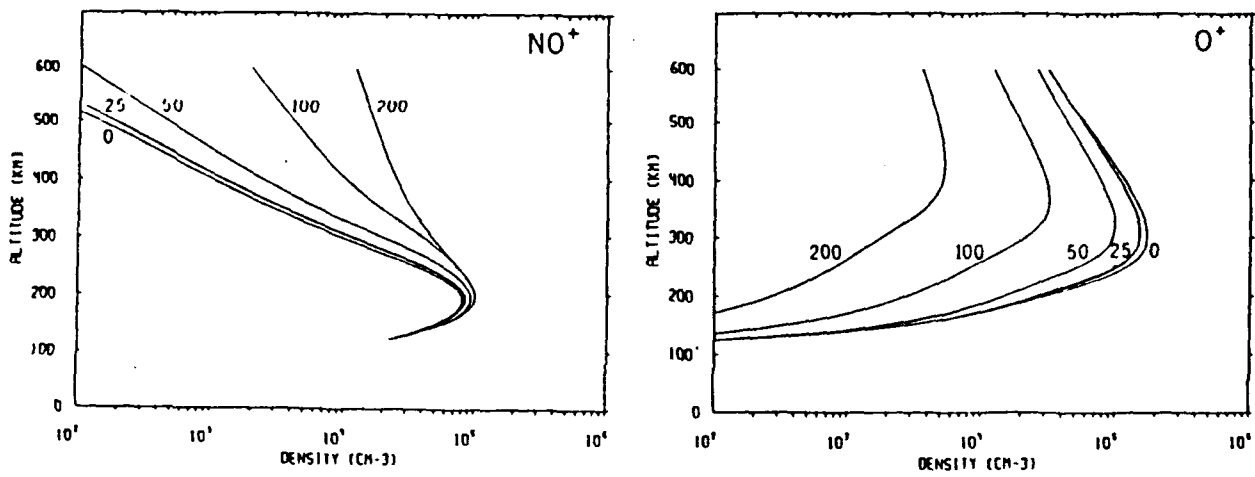


Figure 20. Altitude Profiles of NO^+ and O^+ Densities for Several Effective Electric Field Strengths (mVm^{-1})

Evans et. al., [1983] argued that substorms can play an important part in trough formation. They introduced the concept of a "Fossil Theory" of trough formation, where an increase in the ion-atom interchange (which depends upon the square of the velocity difference between ions and neutrals) could form a trough. It is suggested that during a substorm when the F-region electric fields are on the increase and expand equatorward, along with an accompanying plasma flow increase, a trough can develop extending along paths which pass through regions of rapid plasma flow. A trough created at such a time may be left as a "fossil" or ionospheric signature of the region of fast convective flow as the electric fields diminish following the substorm. It is this ionospheric relic or signature that can later corotate around through the night sector as the electric field subsides, only to be filled in when entering the sunlight on the dawn sector.

When considering trough formation then, the factors which should be accounted for are:

- (i) The stagnation and decay of ionization in flux tubes on the nightside that are slowed or arrested in a sun-earth frame by the combination of convection and co-rotation.
- (ii) The increased recombination rate that occurs in regions of rapid convection.
- (iii) The downward electromagnetic drift introduced when electric fields are eastward.
- (iv) The role of particle precipitation in forming the poleward edge to the trough.
- (v) Upwelling of the neutral atmosphere in regions of intense Joule heating, leading to greater molecular concentrations and faster recombination.

5.0 STATISTICAL STUDIES AND MODELS

Statistical analysis of the main-trough location has been undertaken by a number of workers [Rycroft and Thomas, 1970; Rycroft and Burnell, 1970; Köhnlein and Raitt, 1977]. If Λ_t represents the invariant latitude then some empirical relationships for the location of the center of the trough may be given as:

$$\Lambda_t = 62.2^\circ - 1.6 K_p - 1.35t \quad \text{Collis and Haggstrom [1988]} \quad (1)$$

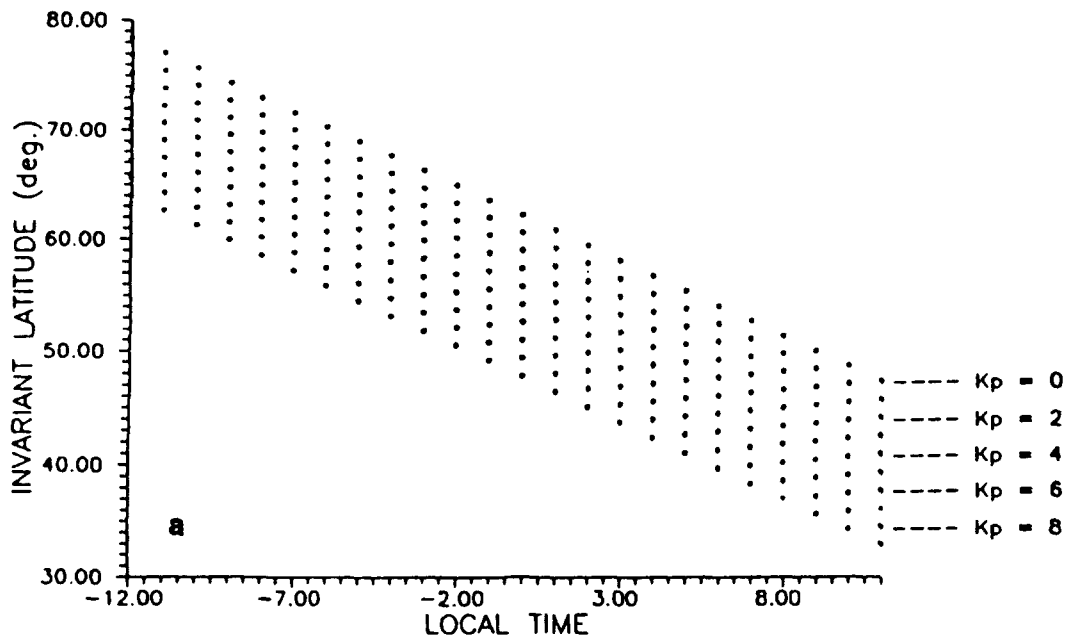
$$\Lambda_t = 65.2^\circ - 2.1 K_p - 0.5t \pm 2^\circ \quad \text{Köhnlein and Raitt [1970]} \quad (2)$$

$$\Lambda_t = 62.7^\circ - 1.4 K_p - 0.7t \pm 3.5^\circ \quad \text{Rycroft and Burnell [1970]} \quad (3)$$

where t represents the local time and is negatively counted before midnight, (i.e. 2300 LT = $t = -1$ hr, etc.). Note that these empirical relations are only applicable from 1900 - 0500 LT.

Using the empirical relations 1, 2 and 3 for the center of the trough position, it was possible to produce graphs of invariant latitude locations as a function of time and K_p . These results are given in Figures 21a, b and 22a. Comparing between empirical relations it is clear that relation (1), derived by Collis and Haggstrom [1988], from data collected during 1986-87 (a period of low sunspot activity), displays the greatest variability in invariant latitude. For a $K_p = 0$ the center of the trough moves from 69° at 1900 LT to 55.5° at 0500 LT. Hence for magnetically quiet days (i.e. $K_p = 0$) the center of the main trough should be located over Goose Bay ($\Lambda = 64.42^\circ$) at around 2200 LT, over Argentina ($\Lambda = 58.03^\circ$) at around 0300 LT and just poleward of Millstone Hill ($\Lambda = 53.92^\circ$) at around 0500 LT.

In comparison, empirical relation (3) derived by Rycroft and Burnell [1970] from data collected during April-August 1963 (a period of low sunspot activity) shows the least variation of all three stations throughout the night. For $K_p = 0$ the center of the trough is located at 66.2° at 1900 LT and 59.2° at 0500 LT. Which means that the center of the trough will be over Goose Bay at around 2200 LT, and just poleward of Argentina at 0500 LT.



TROUGH POSITION : RYCROFT AND BURNELL

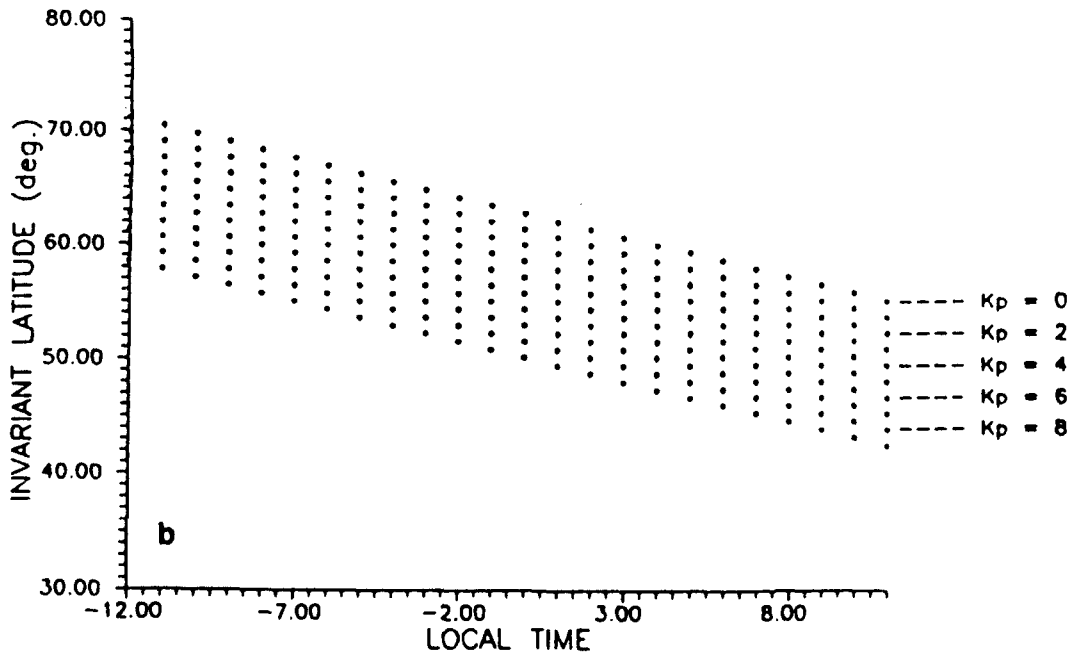


Figure 21. Trough Position, (a) Collis and Haggstrom, (b) Rycroft and Burnell

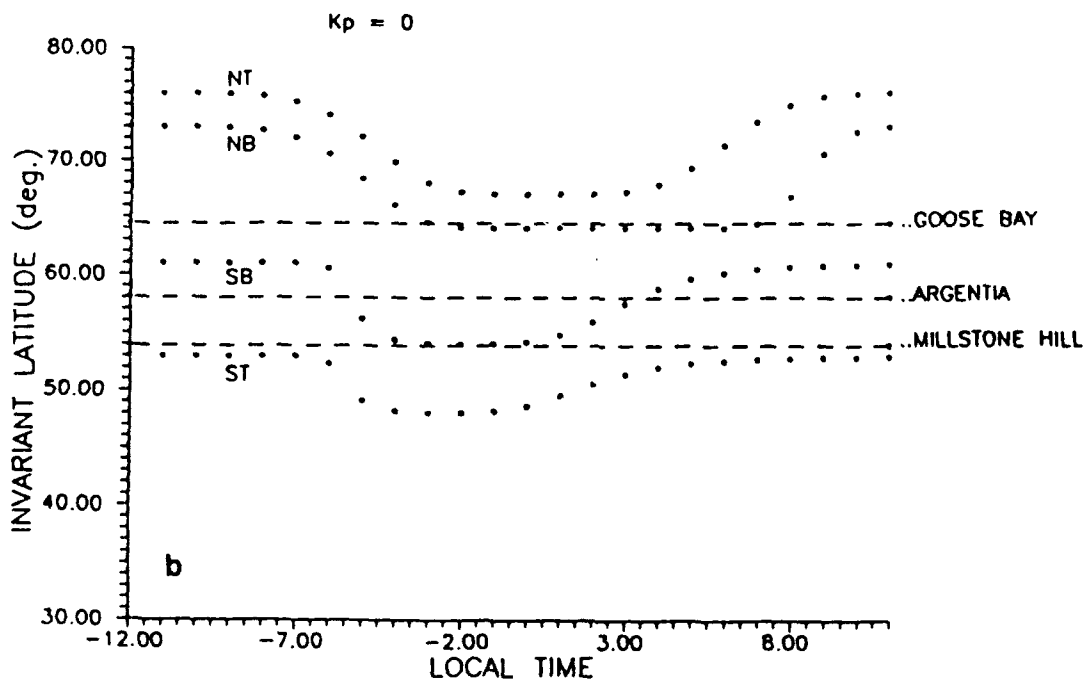
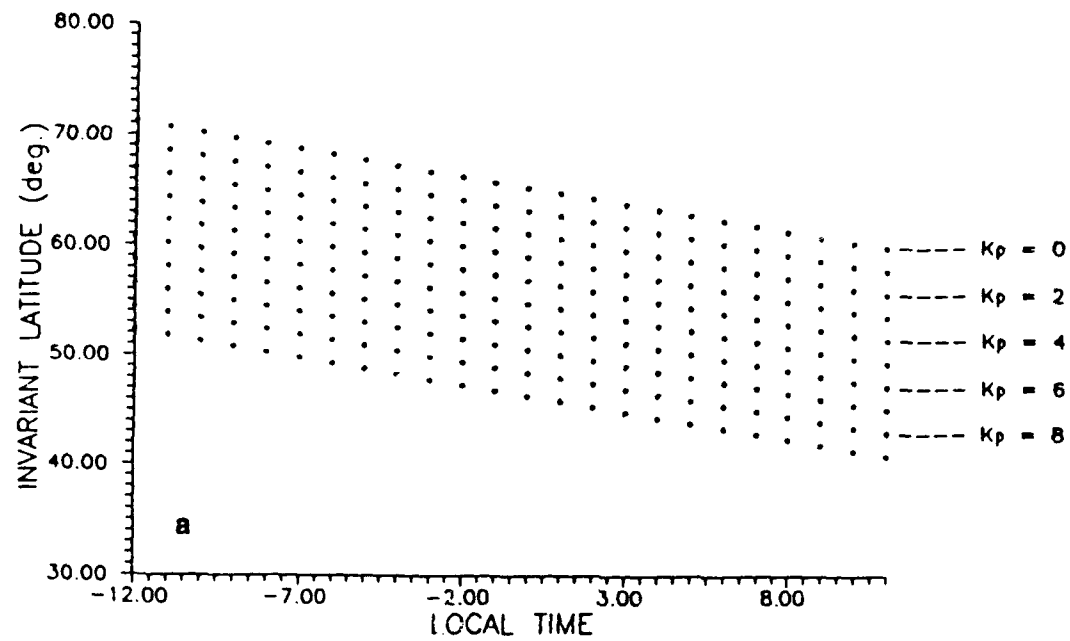


Figure 22. Trough Position, (a) Kohnlein and Raitt, (b) Halcrow and Nisbet

While the diurnal variation in trough location is shown to vary the most using the empirical relation 1, the greatest variation in trough position with increasing Kp is shown by relation 3. At 1900 LT for Kp = 0, the position of the center of the trough is located at 66.2° Λ (Figure 22a). As Kp increases the position of the trough moves to lower latitudes, so that at 1900 LT and Kp = 7, the center of the trough is located at 53.6° Λ, a displacement of 12.2° Λ.

It is clear that for all empirical relations, at Kp values greater than or equal to 4 the trough should be observable at Millstone Hill. However, the discrepancies between these results are large and need to be further investigated. As a test, Millstone Hill data, as well as Goose Bay and Argentia data, may be used to confirm which one of the empirical relations 1, 2 and 3 best describes the location of the main trough.

An alternative set of empirical relations which described the position of the trough walls was outlined by Halcrow and Nisbet [1977]. Using an extensive data base, consisting of 29,770 observations of peak electron densities (measured by topside sounders Alouette I and II from 1962 to 1970), they further extended the analysis of Feinblum [1973] and provided peak electron densities in the trough region, as well as trough location.

Halcrow and Nisbet [1977] presented their results using the ratio Φ where:

$$\Phi = \frac{\text{NmF2 observed}}{\text{NmF2 (CCIR)}}$$

The values of Φ were plotted as a function of the invariant latitude intersections at 300 km. Then these values were used to determine the location of the top and bottom of the trough walls by using a simple model consisting of a linear gradient of the Φ function. Hence the results are not a direct measure of NmF2 but rather its difference to a modelled NmF2. Halcrow and Nisbet [1977] gave the following relations for the main-trough location. Let ST and SB represent the Top and Bottom, respectively, of the south wall (or equatorward wall) of the trough and NT, NB the Top and Bottom of the north wall (or poleward wall) of the trough. The location of the trough may be given in invariant latitude as:

$$\Lambda_{ST} = 48^\circ + 5^\circ \left\{ 1 + \left[1 + \left(\frac{T^2 - 4}{5.6T + 0.1} \right)^{22} \right]^{-0.5} - \left[1 + \left(\frac{T^2 - 8}{12.3T + 0.1} \right)^{14} \right]^{-0.5} \right\} \quad (4)$$

$$-\Lambda_{SB} = 54^\circ - 0.5^\circ (Kp - 1/3) + 7^\circ \left\{ 1 + \left[1 + \left(\frac{T^2 - 4}{5.8T + 0.1} \right)^{22} \right]^{-0.5} - \left[1 + \left(\frac{T^2 - 8}{13.5T + 0.1} \right)^{16} \right]^{-0.5} \right\} \quad (5)$$

$$-\Lambda_{NB} = 64^\circ - 1.0 (Kp - 1/3) + 9^\circ \left\{ \exp(-1.9 \times 10^{-5} T^{5.42}) + \exp(-2.15 \times 10^{-3} (24 - T)^{4.55}) \right\} \quad (6)$$

$$-\Lambda_{NT} = 67^\circ - 1.25^\circ (Kp - 1/3) + 9^\circ \left\{ \exp(-1.7 \times 10^{-5} T^{5.35}) + \exp(-4.66 \times 10^{-4} (24 - T)^{4.1}) \right\} \quad (7)$$

where

$$\begin{aligned} T &= LT + 12 \text{ hr} && \text{if } LT < 12 \\ T &= LT - 12 \text{ hr} && \text{if } LT \geq 12. \end{aligned}$$

The form of the equations presented here are slightly different to the original presentation in Halcrow and Nisbet [1977]. We believe that these equations are now in the correct form. Halcrow and Nisbet [1977] further set restrictions for the sunrise and sunset walls of the trough, where the sunrise wall was specified when the solar zenith angle χ was:

$$\begin{aligned} \chi_{T1} &\leq 95^\circ \pm 1^\circ && \text{Trough begins to fill} \\ \chi_{B1} &= 87 && \text{Trough filled completely.} \end{aligned}$$

At sunset a 1.5 hour lag was introduced so that

$$\chi_{T2} (LT - 1.5) = [87^\circ \pm 3^\circ] - (3^\circ \pm 0.5^\circ) (K_p - 1/3)$$

$$\chi_{B2} (LT - 1.5) = [91^\circ \pm 3^\circ] - (3^\circ \pm 0.5^\circ) (K_p - 1/3)$$

Using relations (4) to (7) it was possible to construct plots of trough position with respect to invariant latitude. Figure 22b shows such a plot for $K_p = 0$, where the south wall top (ST) and bottom (SB) and north wall top (NT) and bottom (NB) of the trough are given as well as the location of the three stations Goose Bay, Argentina and Millstone Hill.

In Figure 22b a distinctive diurnal variation in the location of the main trough exists. This type of variation is not apparent in the previous three empirical relations. Halcrow and Nisbet's [1977] model tends to better represent the diurnal movement of the trough as observed from the statistical analysis presented by Liszka [1967] (Figure 7). In addition it gives an indication of differences between the characteristics of the south and north walls of the trough, since with respect to LT the movement of either wall is uncorrelated. As an example after sunset the south wall of the trough moves to lower latitudes before the north wall of the trough begins to move. Similarly as sunrise approaches the south wall again begins to move to higher latitudes, while the north wall remains stationary for a couple of hours more, and then begins to move to high latitudes. In general the movement of the north wall tends to lag that of the south wall in LT.

For this empirical relation model, at $K_p = 0$ all stations are within the trough boundaries. Further Figures 23 and 24 display the location of the trough walls with increasing K_p , where the south top (Figure 23a), south bottom (Figure 23b), north bottom (Figure 24a) and north top (Figure 24b) walls are given separately. From these figures it is apparent that the north (or poleward) wall of the main trough moves to lower latitudes faster with increasing K_p than does the south (or equatorward) wall. This indicates that if only one main-trough exists, then with increasing K_p , the width of this trough should decrease considerably. Taking as an example the separation in the bottom of the south and north walls at 0000 LT and $K_p = 0$, this is given as $64.0 - 54.2 = 9.8^\circ \Lambda$. While at $K_p = 9$ and 0000 LT the separation is $55.0 - 49.7 = 5.3^\circ$.

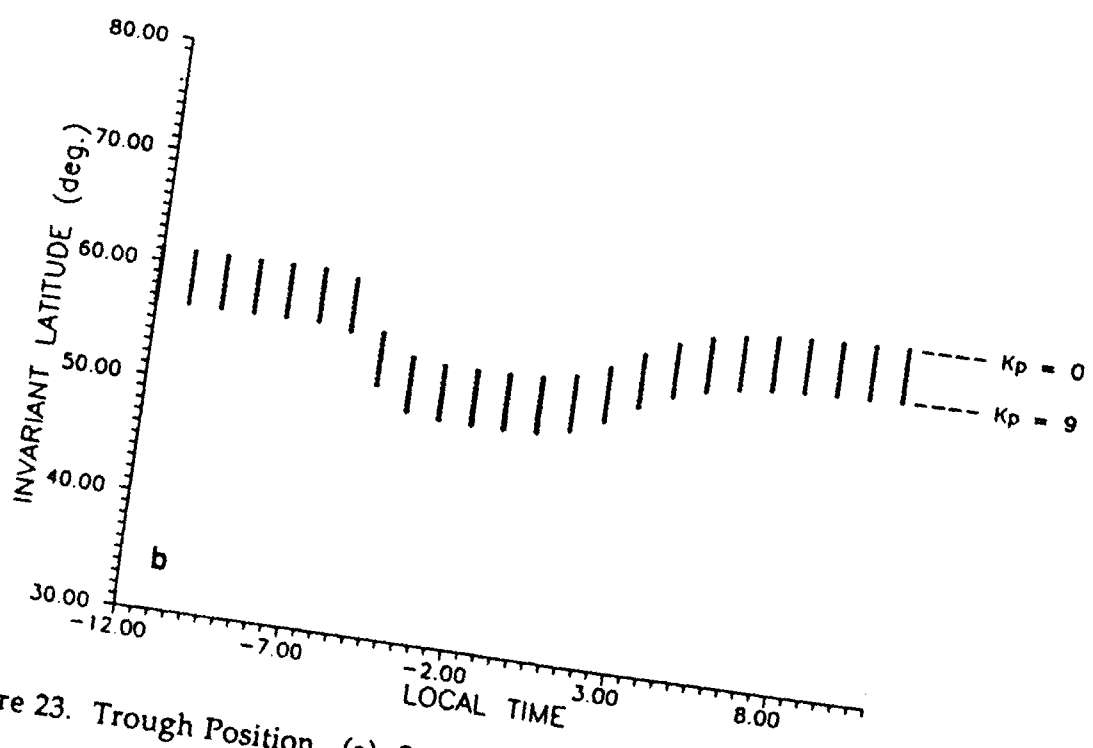
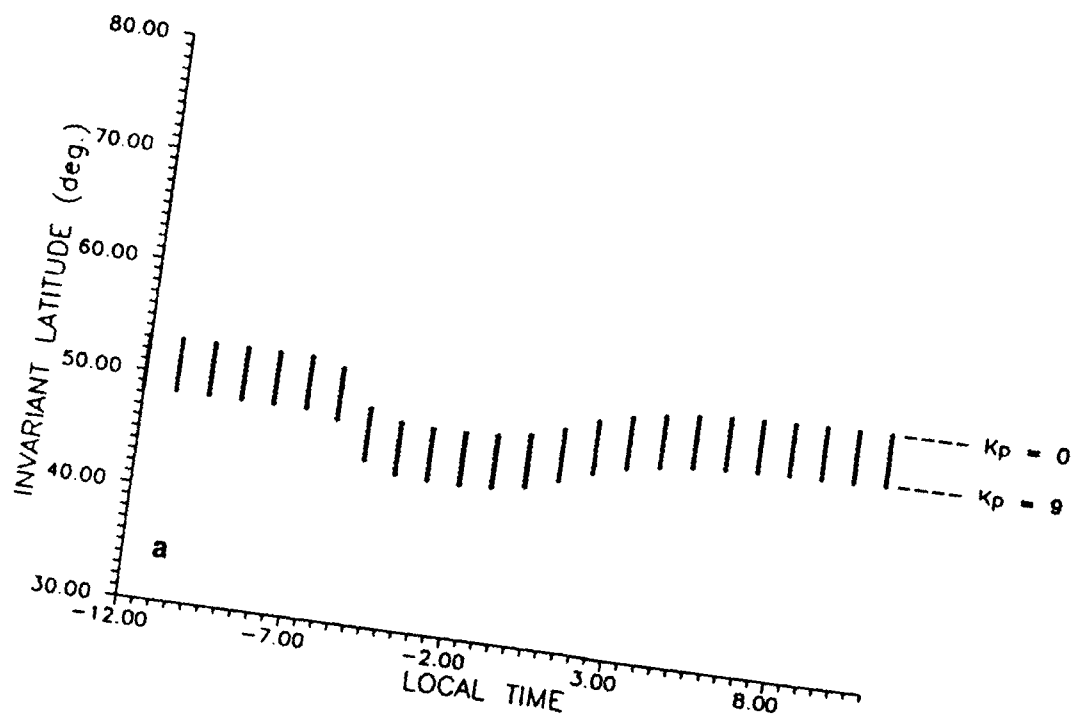


Figure 23. Trough Position, (a) Southern Edge Top, (b) Southern Edge Bottom

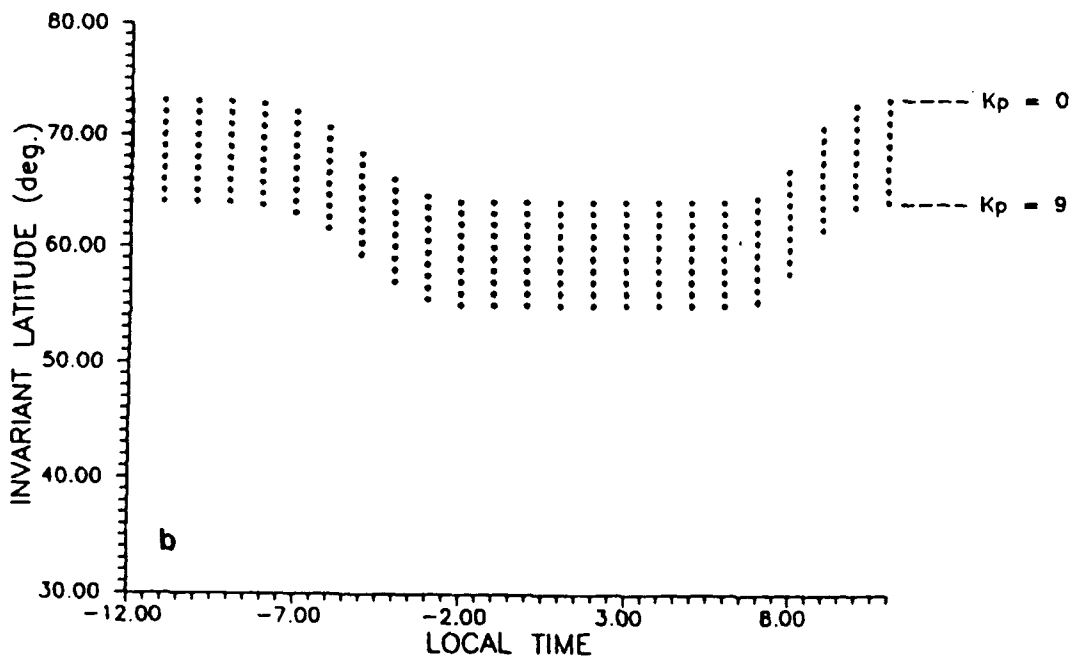
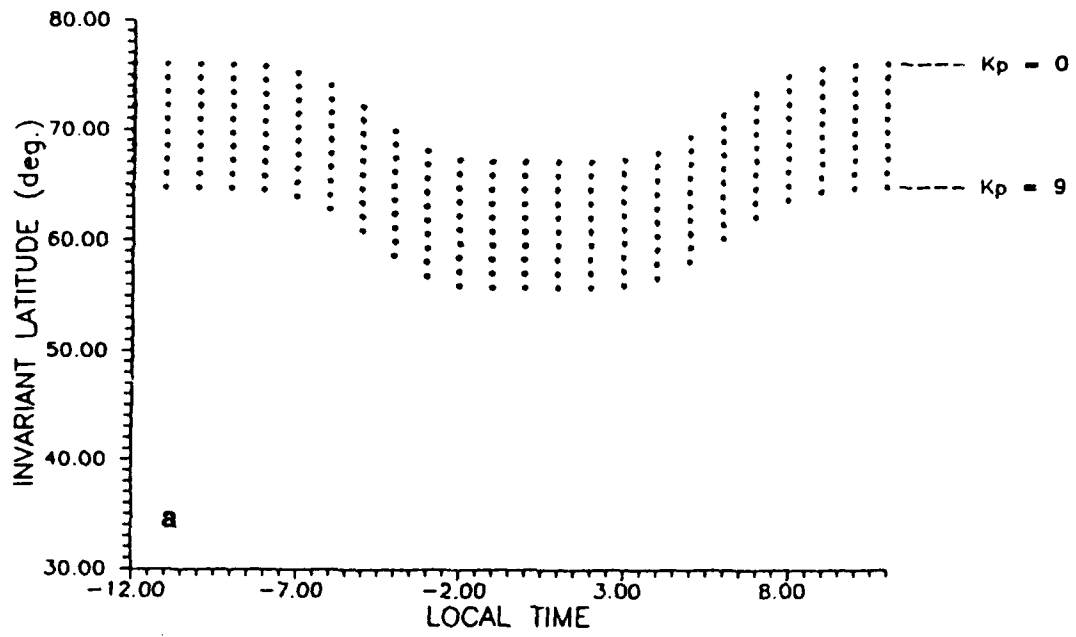


Figure 24. Trough Position, (a) Northern Edge Top, (b) Northern Edge Bottom

In Figures 22b, 23 and 24 the location of the trough has been calculated during day as well as night hours. While the authors tend to place restrictions on these times (since they were interested only in the nocturnal features of the main-trough), for our preliminary analysis its best to illustrate where the main-trough would be located if it did not fill in during the day. However, the location of the main-trough during daylight hours should not be mistaken for the so-called daytime trough. While the daytime trough can overlay the location of the main trough in the pre- and post-noon sectors, the two troughs are unrelated because of different source mechanisms.

The main trough as mentioned previously may be a result of plasma stagnation in the dusk sector. The dayside trough, however, arises from the auroral oval moving to larger solar zenith angles at times when the magnetic pole is on the anti-sunward side of the geographic pole [Sojka et al., 1985]. Then as the auroral ionization recedes, a region of declining photo-ionization is left on the dayside which results in the formation of a dayside trough.

5.1 Electron Temperature Enhancements in the Main-Trough Region

Using the Alouette 2 satellite Norton and Findley [1969] observed an electron temperature enhancement that occurred along the magnetic field-line in the region of the main trough. The enhanced electron temperature was considered to be due to heat conduction from the plasmasphere where the electron energy is higher than in the ionosphere.

Watanabe et. al., [1989], using data collected from the Ohzora satellite, also showed the existence of a heat flux from the magnetosphere to the ionosphere along the magnetic field-line in the trough region. It was observed that when the probe faced to the direction of ground along the magnetic field-line, the electron temperature increased. In addition Watanabe et al. [1989] also discussed the existence of a double peak in electron temperature enhancement within the trough region. This double peak would be more pronounced during high magnetically active periods. In general the distance between the two peaks is about 2-3° magnetic latitude when examples of the double peak are given in Figure 25 (reproduced from Figure 2 in Watanabe et al. [1989]).

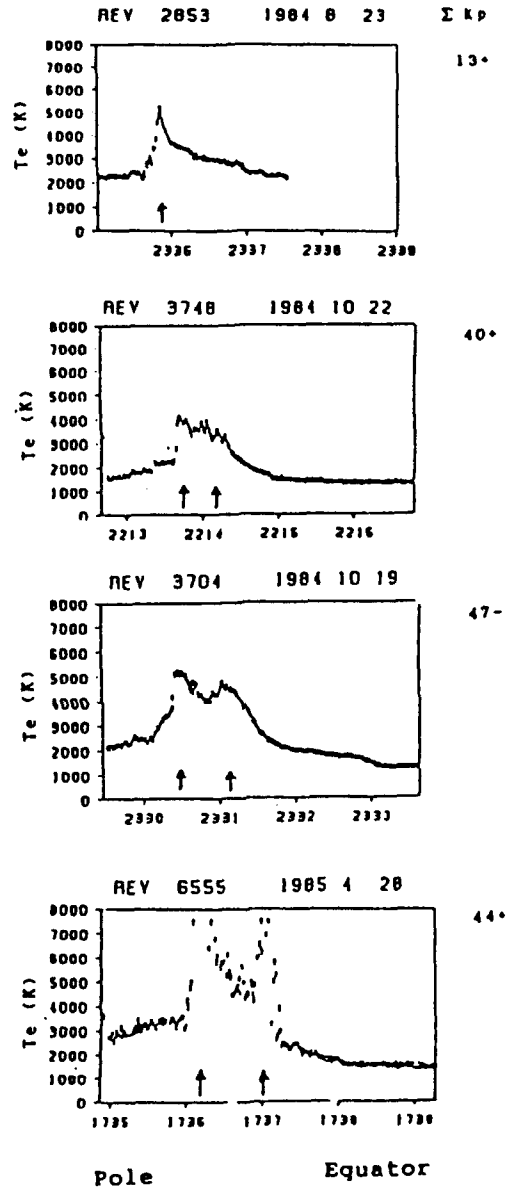


Figure 25. Structure of Electron Temperature in the Ionospheric Trough Region. The Peak of the Electron Temperature is Indicated with an Arrow. The Double Peaks of the Electron Temperature Appeared in the Magnetically Active Periods and the Distance Between Two Peaks was Large in These Periods.

5.1.1 Problems Encountered with Trough Measurements

The problems that have been encountered with trough studies in the past may be listed as:

1. Widely varying altitudes of measurements.
2. Use of limited data base.
3. Varying spatial resolutions of the measurements from a few km to nearly 1000 km.
4. Difficulties in detecting dayside features due to photoelectrons.
5. Varying criteria used to define the trough location.
6. Uncertainties in the convection electric field.
7. Uncertainties in the positioning of the auroral particle source of ionization.
8. Uncertainties in the abundance of excited nitrogen molecules in the trough region.
9. Insufficient data to delineate small features in the structure at the bottom of the trough.

5.1.2 Physical Processes that Should be Considered for Trough Formation

Throughout the analysis processes that need to be addressed in order to explain trough formation and characteristics can be listed as:

1. Plasma convection, i.e.
 - a) Vertical velocities inside and outside the trough boundaries may give a good representation on how convection patterns are influencing the shape of the trough.
 - b) Rapid ion convection due to electric fields increase the ion temperature T_i by the heating of ion-neutral friction [Schunk and Sojka, 1982].
 - c) Depleted plasma tubes formed in the nightside are convected westward to the afternoon sector where they are observed as pre-dusk troughs [Spiro et al., 1978].

d) Competing eastward and westward plasma convection produces a Stagnation region in which a trough is formed.

2. Ion Chemistry.
3. Recombination Rates.
4. Plasma escape.
5. Neutral air winds.

Transport of excited N₂ molecules by equatorward wind speeds (electric fields or ion convection speeds) of 100 m/s can increase recombination rates and produce deeper troughs [Schunk and Banks, 1975].

6.0 USING THE AIR FORCE HIGH LATITUDE DIGISONDE NETWORK FOR TROUGH STUDIES

In investigating the characteristics of the main trough, the Air Force high latitude Digisonde Network was used. In particular, data gathered from the stations, Goose Bay, Argentia and Millstone Hill (over the six month period from January to June 1990) has been analyzed and forms the major part of these investigations. As mentioned in a previous section, the stations Goose Bay, Argentia and Millstone Hill are located near the main trough, and during periods of increasing magnetic activity, offer the best opportunity in observing the movement of the main trough to lower latitudes.

In the analysis of the characteristics of the main trough consideration will be given to a few points that have not been extensively addressed in previous observations. These points may be listed as;

1. Plasma motion and the extent of trough formation will be correlated.
2. Trough variability from day-to-day, e.g. how long after an increase in Kp does it take for a trough to appear at lower latitudes, and how long does it take to move back to higher latitudes.
3. Convection: Since it is believed that the pre-midnight main trough results from plasma stagnation in the dusk sector, the eastward and westward convection patterns must be considered.

By using the Drift mode capabilities of the Digisonde systems at Goose Bay, Argentia, Millstone Hill and comparing the convection patterns observed during magnetically quiet and disturbed periods, it is possible to statistically determine the dependence of trough formation on "local" convection patterns. The next section will describe the procedures used in these investigations. At a later stage when the characteristics of the main trough are better understood, more stations at higher latitudes will be incorporated into the analysis, in particular Sondre Stromfjord and Narssarssuaq. In addition further analysis conducted using oblique ionograms received at Goose Bay and transmitted from Wallops Island, during the month of August 1990. Vertical incidence ionograms from Goose Bay, Argentia and Millstone Hill recorded

during August 1990 will be used to identify troughs, and these time periods will in turn be used to observe what ionospheric signatures the main trough causes on the oblique ionograms.

6.1 Data Handling Procedures

The following is an outline of the procedures adopted to investigate the main trough.

1. For the three most quiet days for each month (low Kp) produce foF2 and hmF2 diurnal variation plots (hopefully when no trough is detected). List these averages as the normal diurnal behavior at each station. Then by comparing the diurnal variation for each day of the month to the average, troughs may easily be identified. As an example, Figure 26a displays the diurnal variation of foF2, hmF2 and the horizontal and vertical velocity components observed on day 044 1990 at Millstone Hill. Universal time is displayed on the horizontal axis at the bottom of the plots. All velocities were calculated for corrected geomagnetic coordinates. The first plot displays the vertical velocity component of drift, labelled Vz on the extreme right-hand side, showing velocities from -40 to 40 m/s. Error bars are included and represent one standard deviation away from the mean. The second plot displays the horizontal velocity component "Vh" as a vector which always starts on the central line. The angle identification code is given on the extreme right by the N(orth), W(est), S(outh) and E(ast) characters. The magnitude of these vectors may be scaled from the scaling vector on the extreme left whose entire length represents 200m/s. As an example, at 1314UT three vectors are displayed. These vectors have been enlarged and appear to the left of the graph. The middle vector represents the mean Vh component, while the outer two vectors display the upper and lower error limits both in magnitude and direction.

The third plot displays the monthly quiet day average and the current day diurnal variation in foF2, in MHz. The last plot displays the monthly quiet day average and the current day diurnal variation for hmF2, in km. Day 044, 13 February 1990, shown in Figure 26a had a sum of Kp of 13-, and was included in the three magnetically quiet day average for that month. So the quiet day average and the daily variations are close. Figure 26b however displays the diurnal variations for

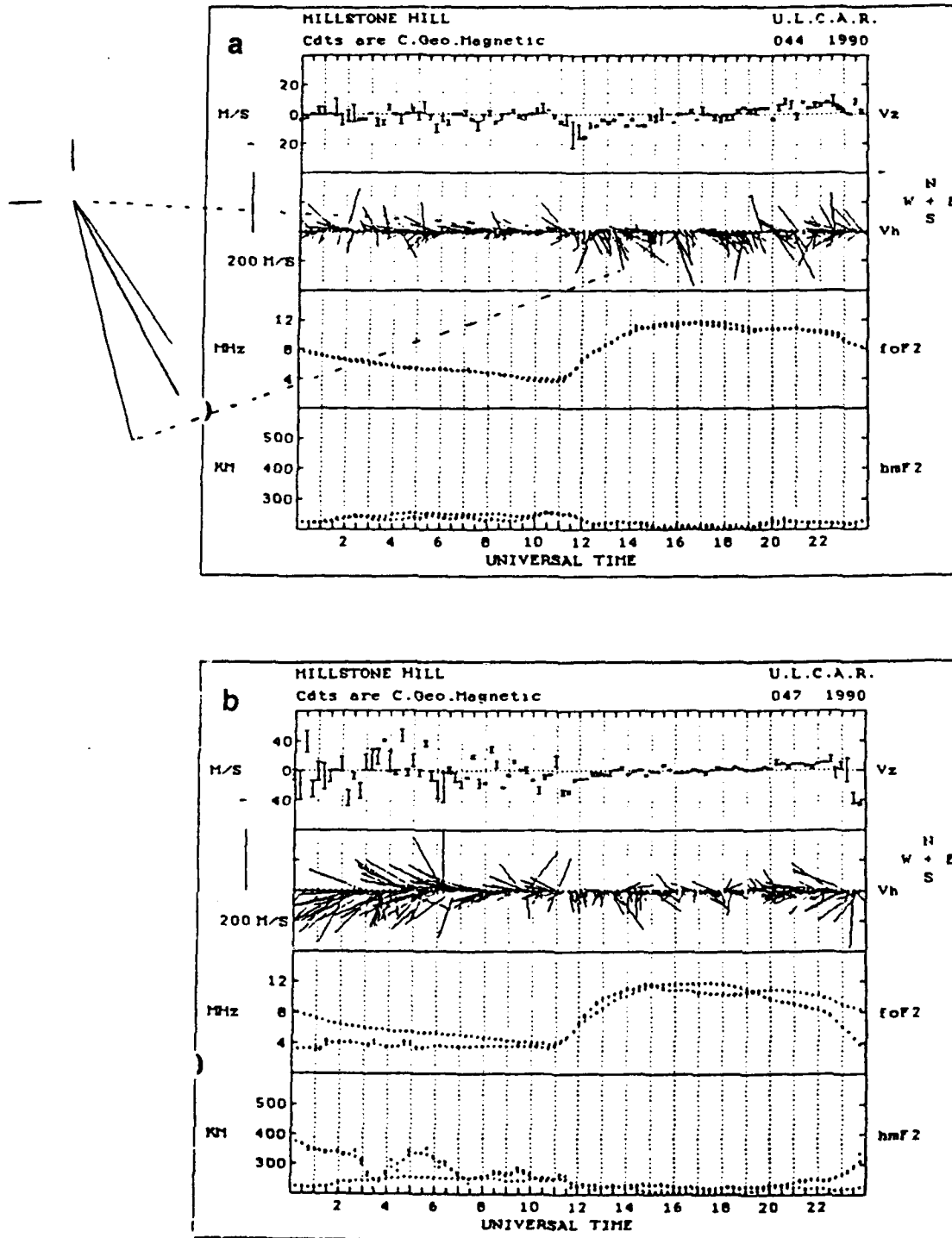


Figure 26. Linear Diurnal Variation Plots for V_z , V_h , f_oF2 and h_mF2 .
 (a) Variations on Day 44 1990 at Millstone Hill for Low K_p Values.
 (b) Variations on Day 47 1990 at Millstone Hill for High K_p Values When a Trough was Detected.

day 047 or 16 February 1990, when the sum of Kp was 38-. It is clear that in Figure 26b troughs are detected both in the night and evening sectors, since foF2 drops to lower values than the monthly quiet day average, and hmF2 increases at times reaching heights 150 km higher than normally observed for quiet time variations.

The plots shown in Figure 26 are good indications that using this setup troughs may be easily identified and drift velocities compared. Further combining the observations from all three stations, Goose Bay, Argentina and Millstone Hill into a polar plot, comparisons of the ionospheric behavior may be made directly. Figure 27 displays a combination of polar plots produced for day 017 1990 when Kp = 17 (moderate magnetic activity).

Figure 27a displays foF2 values for each station, with Goose Bay represented by the inner most circle, then Argentina and Millstone Hill. Figure 27.1a is an enlargement of a portion of Figure 27a.

Figure 27b displays hmF2 values for each station. Figure 27.2b is an enlargement of a portion of Figure 27b.

Figure 27c displays Vh component whose lengths are determined by the scale on the right of the plot and is given in units of 200m/s.

Figure 27d displays Vz component scaled to 50m/s. Vectors pointing from the station's Corrected Geomagnetic latitude radially inwards towards the pole represent negative velocities, while those pointing radially outwards indicate positive velocities.

The example given in Figure 27 displays Vh and Vz group velocities for 5 minute observation periods. It is planned to average the data over 15 minutes to reduce the congestion and allow the detection of variations in the convection patterns. It is clear from Figure 27.1a, b that a trough is present at Goose Bay at approximately 2000 CGLT, since a rapid fall in foF2 and rise in hmF2 are observed. Although Goose Bay consistently displays larger velocity components than is observed at either Argentina, or Millstone Hill, the consistency of the large Vh vectors at around 2000 CGLT and the large positive Vz vector velocities prior to 2000 CGLT are characteristics of the dusk main trough which are commonly observed at Goose Bay and Argentina.

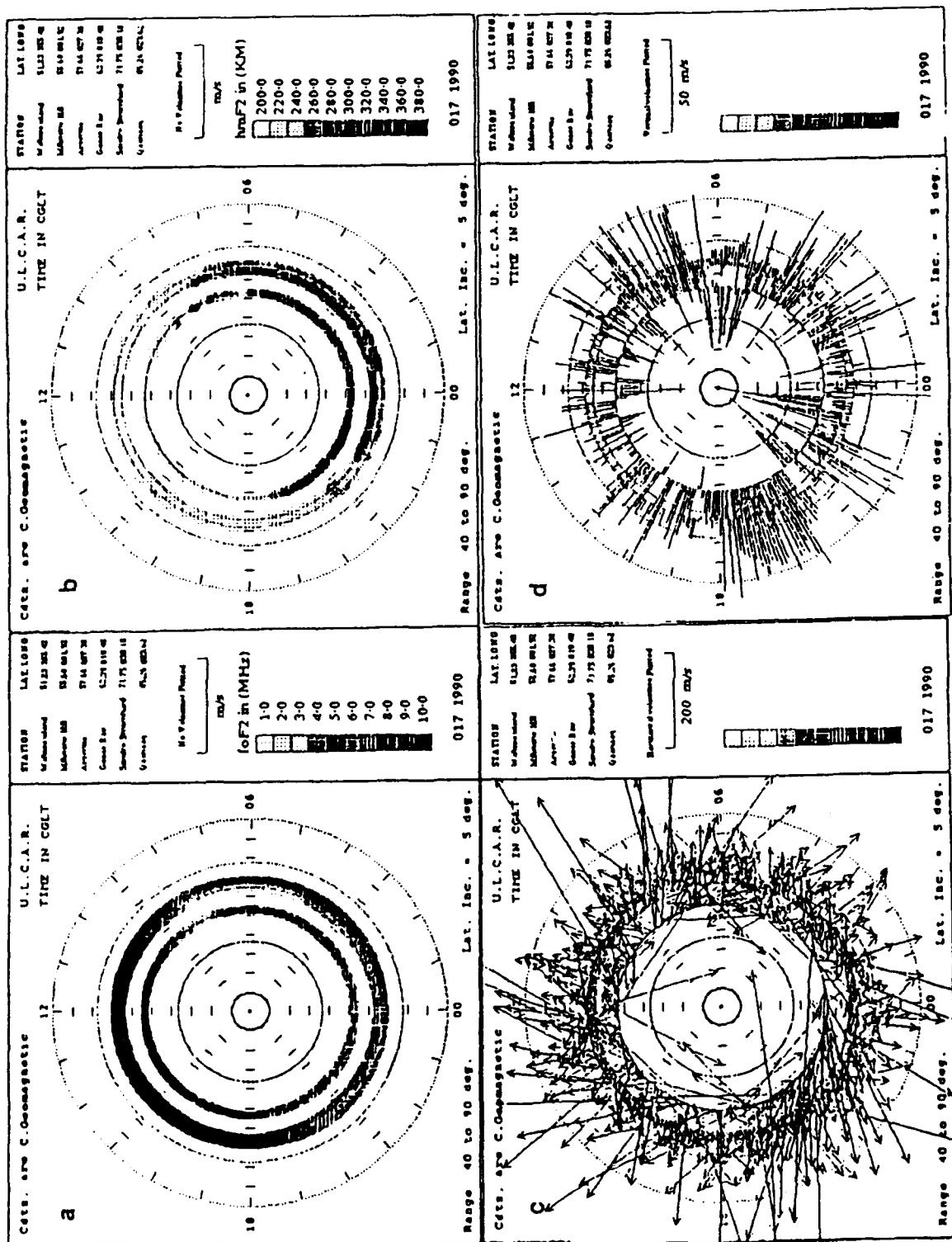


Figure 27. Polar Plots of (a) foF2, (b) hmF2, (c) Horizontal Velocity, Vh and (d) Vertical Velocities, Vz.

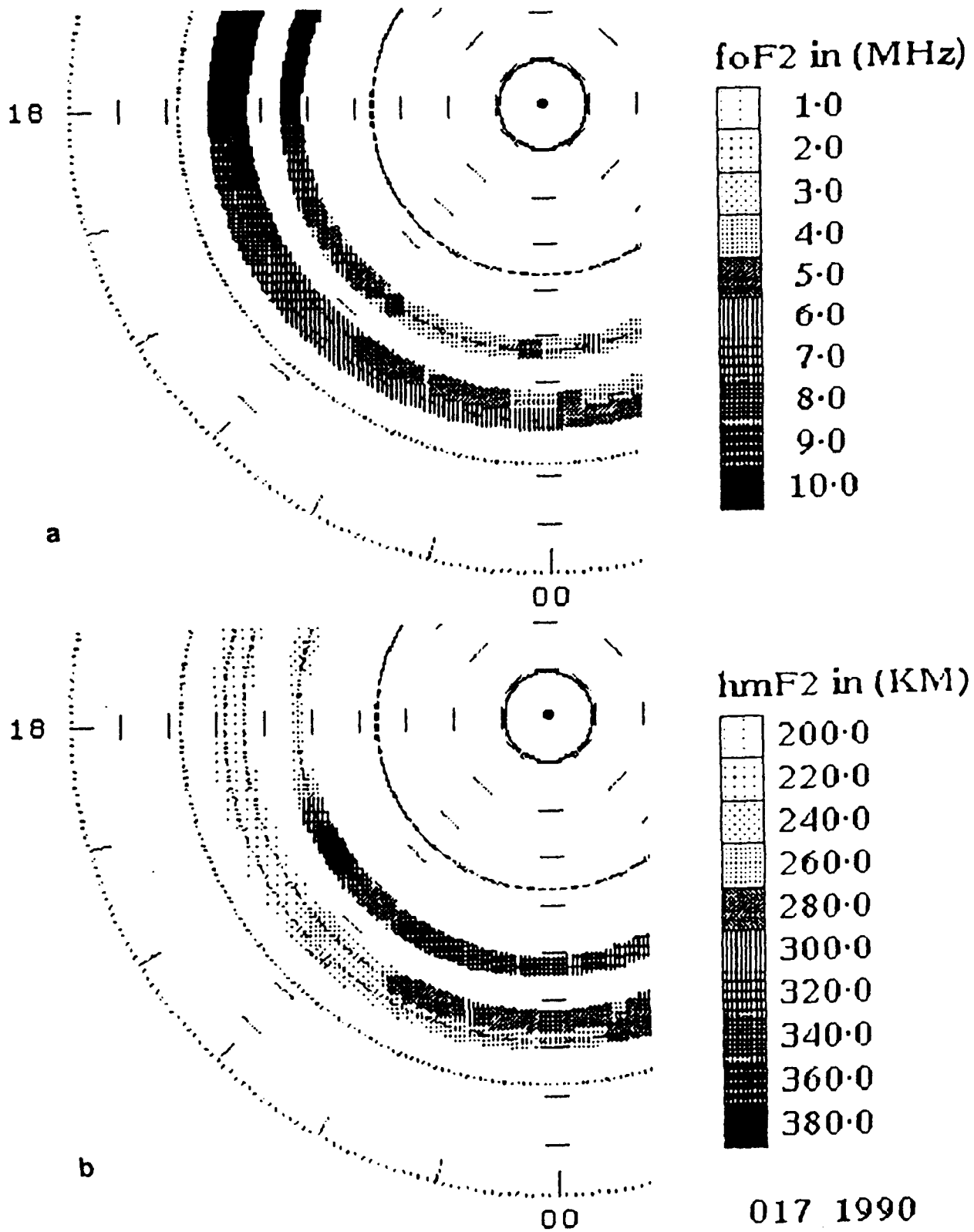


Figure 27.1. Enlarged Dusk Sector from Figure 27 Showing a Trough Detected at Goose Bay. (a) foF2 values and (b) hmF2 values.

2. Data must also be collected in groups of Kp values to determine trough positions and convection characteristics at these high latitude stations. To do this a two year Sum of Kp data base was used to statistically construct the following table.

e.g. Quiet days :	Sum of Kp	($\sum Kp$)	$\leq 8+$
Moderate days :	" " "	$8+ \leq \sum Kp \leq 180$	
Minor storm levels :	" " "	$180 \leq \sum Kp \leq 26+$	
Storm levels	" " "	$270 \leq \sum Kp \leq 35+$	
Major storm levels	" " "	$\sum Kp > 35+$	

3. To begin a statistical data base on the results obtained at each station, ratio plots of the difference between normal diurnal variations and variations observed at different Kp groupings would need to be produced. This data would best be represented by contour plots of the ratio ΦF which is given as:

$$\Phi F = NmF2 (\text{observed}) / NmF2 (\text{normal, low Kp}).$$

Some of these results for the month of March 1990 are given in Figures 28, 29 and 30. Figure 28 shows results obtained from Millstone Hill. Figure 28a displays foF2 ratios, while Figure 28b displays hmF2 ratios. In this representation troughs can be detected on days 071 starting at 2200 UT and still observable on days 072 and 073 at around 0100 UT. Also on day 080 starting at around 0100 UT and on 089 at around 0400UT.

Figure 29 shows results obtained at Argentina. Similarly to those observed at Millstone Hill, troughs are detected on days 073 and 080. The lack of observed troughs on day 71 and 72 at Argentina is due to no data being recorded on these days. These troughs also display the characteristic double peak rise in hmF2 clearly seen at around 0100 UT and then at 0800 UT on day 080, which is a consistent feature of the main trough detected at these stations. Figure 30 shows results obtained at Goose Bay. In comparison to Figures 28, and 29 foF2 and hmF2 ratios at Goose Bay displays a considerable difference. Goose Bay tends to detect troughs before 0000 UT while Argentina and Millstone Hill tend to detect troughs generally after 0000 UT. In addition when the Sum of Kp is high enhancements in the normal nighttime foF2 values are observed, which indicates at these times an extra source of ionization

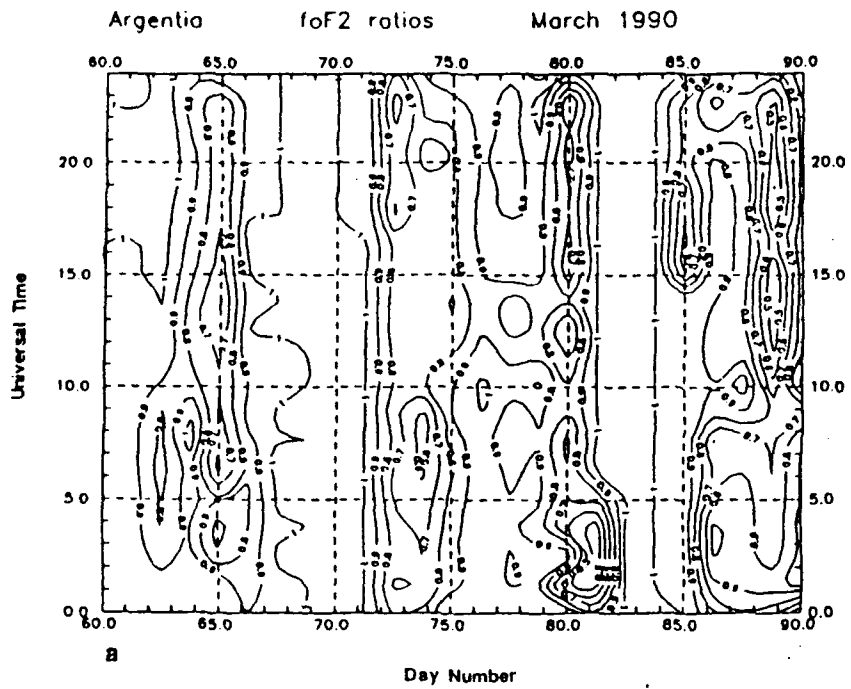


FIGURE.29

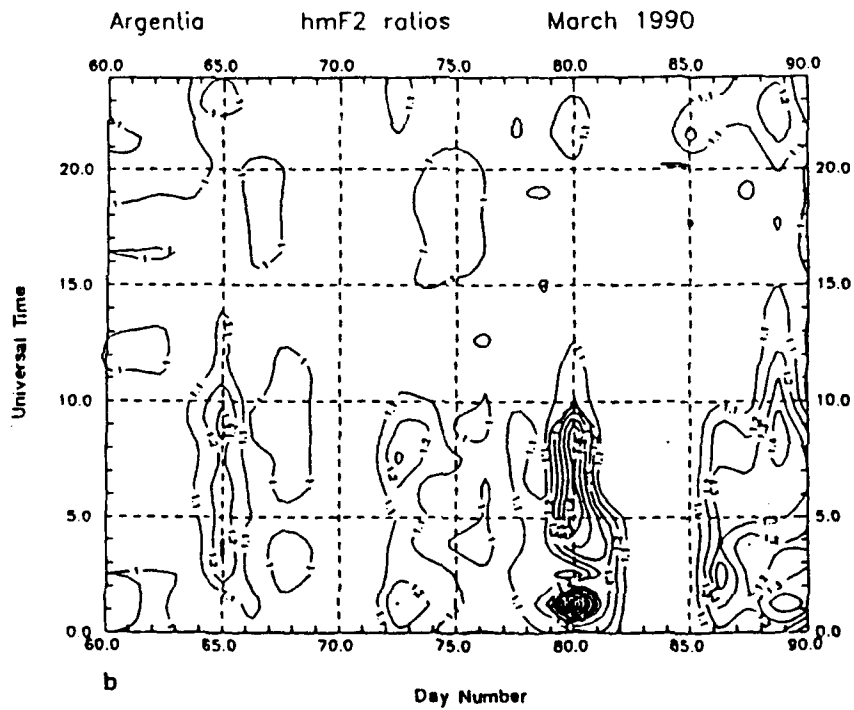


Figure 29. Contour Plots for the Ratio "p" of Observed to Quiet Day Average for the Month, March 1990 at Argentina (a) Represents the pfoF2 ratio, (b) Represents phmF2 ratio.

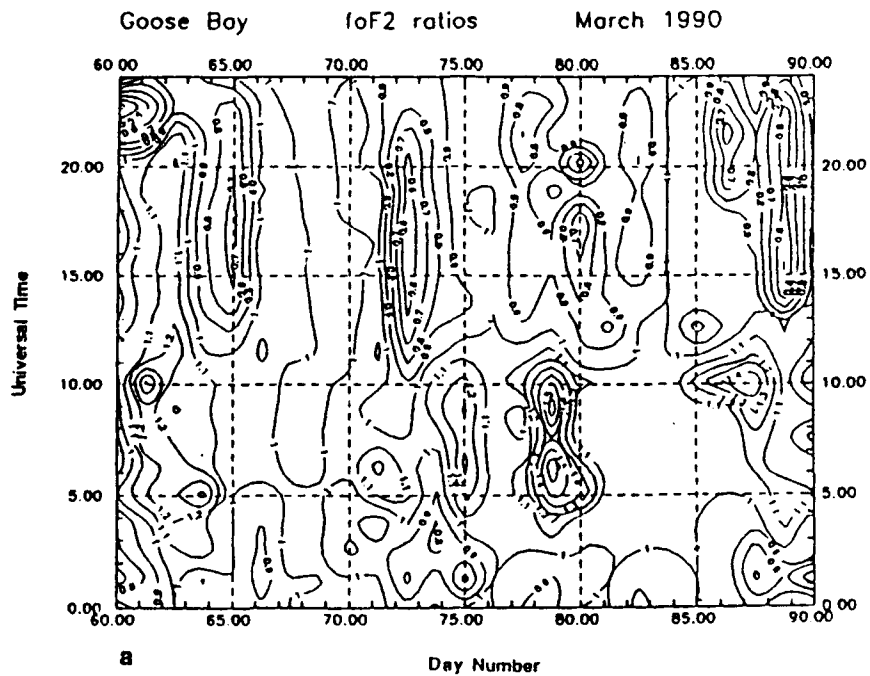


FIGURE.30

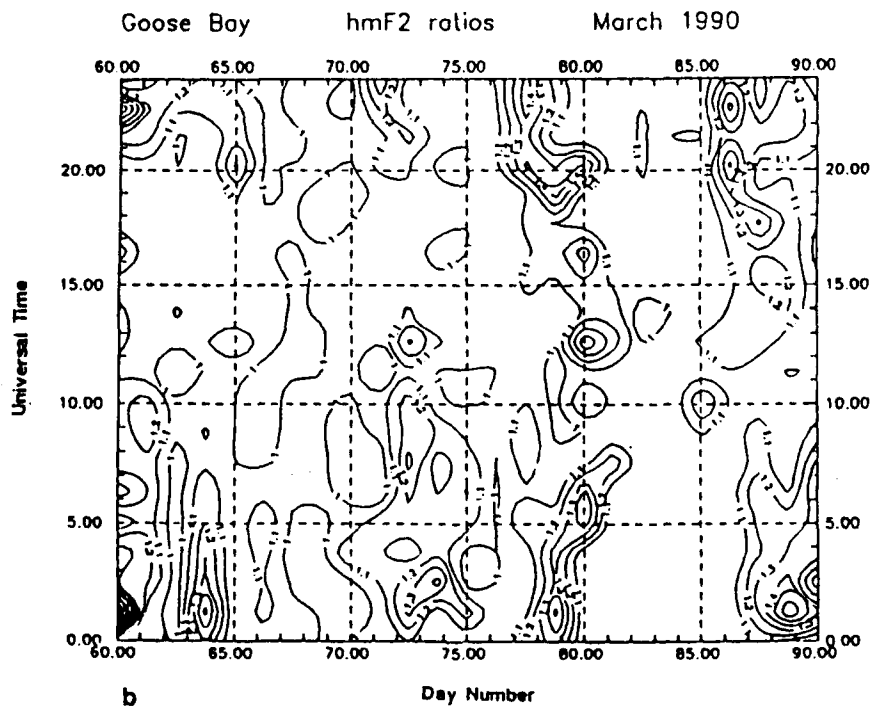


Figure 30. Contour Plots for the Ratio "p" of Observed to Quiet Day Average for the Month, March 1990 at Goose Bay (a) Represents the pfoF2 ratio, (b) Represents phmF2 ratio.

exists. This behavior is consistently observed at Goose Bay yet is almost never seen at the lower latitude stations of Argentinia and Millstone Hill. Similar contour plots are currently being generated for the months of January to June 1990.

4. A similar comparison should be carried out for velocity vectors, i.e. the diurnal variation in plasma motion can be compared to the convections observed during magnetic storms.

5. As well as the statistical samples, individual trough cases are considered. These cases first detected from foF2 and hmF2 results are further analyzed for more detail structure. As an example Figure 31 displays a sequence of ionograms recorded at Millstone Hill, covering the period 0044 to 0644 UT, on day 048 1990. During this period a trough was detected over the station where the minimum in foF2 was observed at around 0159 UT. The reproduction of this figure removes the clarity of certain traces displaying different line of sight Doppler shift values, which are clearly distinguishable in the original color copy. However the example in Figure 31 does indicate that a new leading edge develops in the ionogram at around 0159 UT, where strong echoes are returned at frequencies up to 7.0MHz.

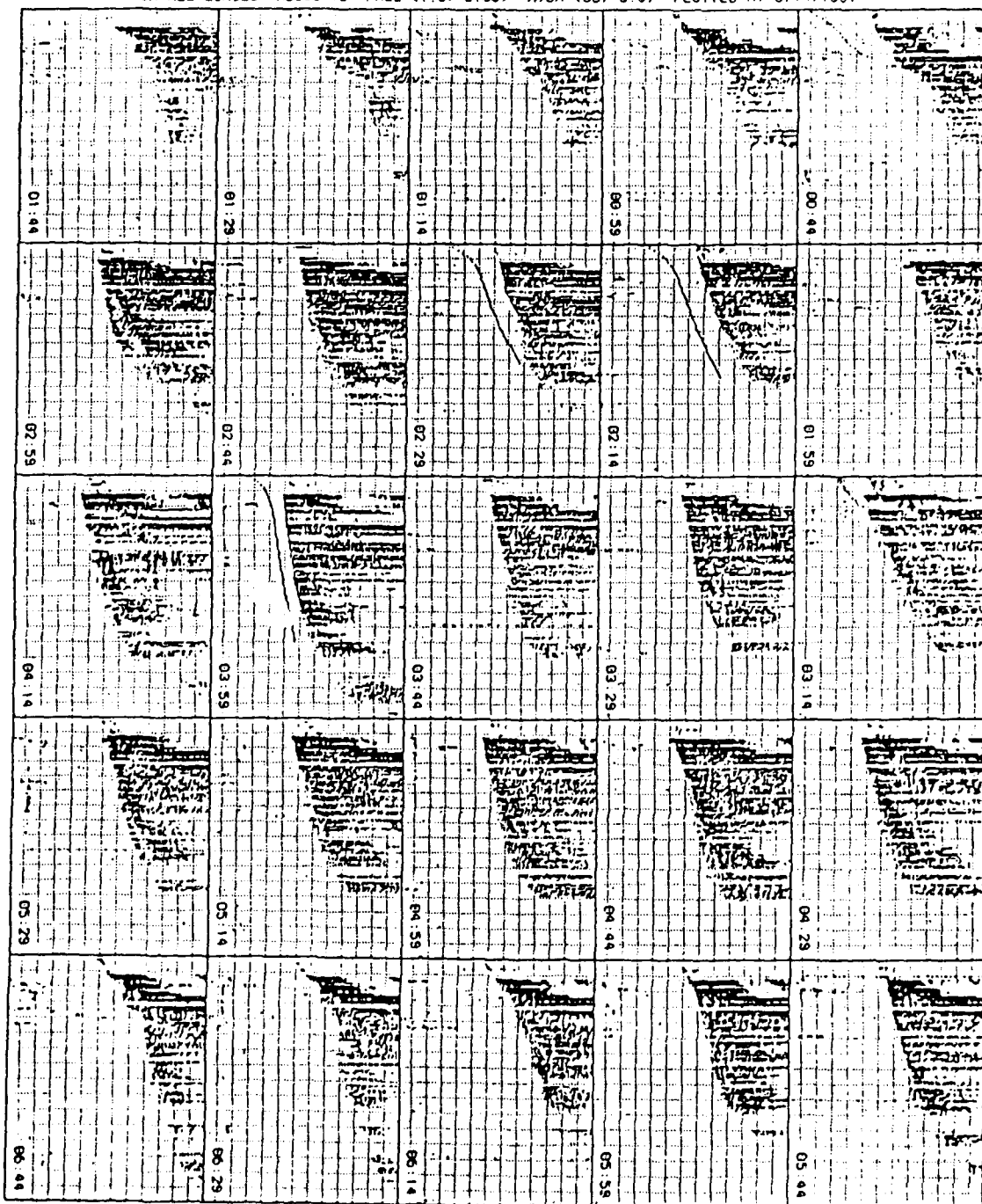
Using the drift mode, "skymaps" were generated for this observation period. A sequence of skymaps are given in Figure 32. For this data one frequency was selected automatically and 64 spectral lines at four height gates were recorded, (this group of data is referred to as one drift case). Each skymap displays the reflection source location points collected over 11 drift cases. In the map the north direction is directly up the page, while west is to the right of the map. The maps are scaled in 5 degree increments with a maximum zenith angle of 60 degrees. The period covered is 0334 Ut where 50 sources are listed, to 0404 UT where 44 sources are listed.

At 0345 UT echoes are primarily returned from two regions, one located at a zenith angle of 30 degrees to the north, and the other at 15 degrees to the south. At around 0400 UT however echoes are only returned from the north. Few echoes are returned from directly overhead when the trough was close to the station. With the use of skymaps the spatial characteristics of troughs will be studied in more detail.

0000

STATION YEAR DOO HMMH OUT PUT FREQ CAB XLZT HAW HEIG UUU PP (42 6N 288 5E)
MILLSTONE HILL 1990 048 0044 1084100 01110 32E 4101 534 123D 042 R2 48 (FEB 17)
FOR ALL ECHOES ADJUST:0 FREQ (1.0, 0.05) HIGH (60, 5.0) PLOTTED AT 5/14/1991

WLCAR



COLOR CODE 0000 0001 0002 0003 0004 0005 0006 0007 0008 0009 0010 0011 0012 0013 0014 0015 0016 0017 0018 0019 0020 0021 0022 0023 0024 0025 0026 0027 0028 0029 0030 0031 0032 0033 0034 0035 0036 0037 0038 0039 0040 0041 0042 0043 0044 0045 0046 0047 0048 0049 0050 0051 0052 0053 0054 0055 0056 0057 0058 0059 0060 0061 0062 0063 0064 0065 0066 0067 0068 0069 0070 0071 0072 0073 0074 0075 0076 0077 0078 0079 0080 0081 0082 0083 0084 0085 0086 0087 0088 0089 0090 0091 0092 0093 0094 0095 0096 0097 0098 0099 0100

Figure 31. Sequence of Ionograms Recorded at Millstone Hill When a Trough was Present.

SKYMAP SURVEY

Station 042 Date 90 048 Time (UT) 03:34:09 OUTPUT 00A410C XLZT 0B20 NRW 525 HE16 0000 Zmax 60.0 M= 5 V= 10 T= 0dB

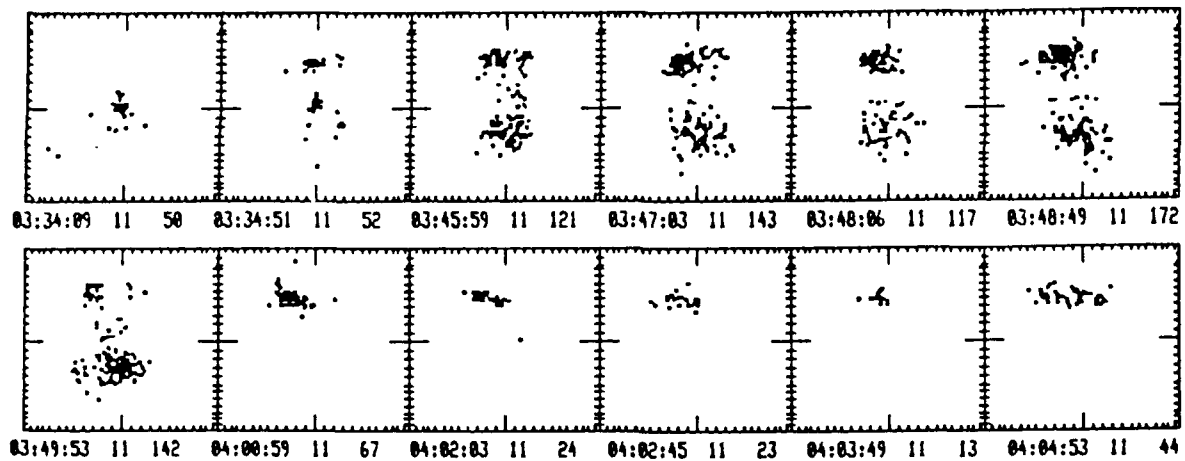


Figure 32. Sequence of Skymaps for Day 48 1990 at Millstone Hill.
Each Map Combines 11 Subcases.

7.0 REFERENCES

- Ahmed, M., Sagalyn, R.C., Wildman, P.J.L. and Burke, W.J., "Topside ionospheric trough morphology; Occurrence frequency and diurnal, seasonal and altitude variations," *J. Geophys. Res.* Vol. 84, pp489-498, 1979.
- Banks, P.M., Shunk, R.W. and Raitt, W.J., "NO⁺ and O⁺ in the high latitude F-region," *Geophys. Res. Lett.* Vol.1, pp239-242, 1974.
- Bowman, G.G., "Ionization troughs below the F₂-layer maximum," *Planet. Space Sci.* Vol.17, pp777-796, 1969.
- Brace, L.H. and Theis, R.F., "The behavior of the plasmopause at mid-latitudes; ISIS 1 Langmuir probe measurements," *J. Geophys. Res.* Vol. 79, pp1871-1884, 1974.
- Brace, L.H., Theis, R.F. and Hoegy, W.R., *Geophys. Res. Lett.* Vol.9, pp989, 1982.
- Brinton, H.C., Grebowsky, J.M. and Brace, L.H., "The high-latitude winter F-region at 300 km; thermal plasma observations from AE-C," *J. Geophys. Res.* Vol. 83, pp4767-4776, 1978.
- Carpenter, D.L., "Whistler studies of the plasmopause in the magnetosphere," *J. Geophys. Res.* pp693-709 1966.
- Carpenter, D.L. and Park, C.G., "On what ionospheric workers should know about the plasmopause-plasmasphere," *Rev. Geophys. Space Phys.* Vol. 11, pp133-154, 1973.
- Chacko, C.C., "The high-latitude behavior of hmF₂ and NmF₂ along the noon-midnight meridian under quiet conditions," *J. Geophys. Res.* Vol. 83, pp5733-5736, 1978.
- Chappell, C.R., "Recent satellite measurements of the morphology and dynamics of the plasma-pause," *Rev. Geophys. Space Phys.* Vol. 10, pp951-979, 1972.
- Collis, P.N. and Haggstrom, I., "Plasma convection and auroral precipitation processes associated with the main ionospheric trough in high latitudes," *J.A.T.P.*, Vol.50, pp389-404, 1988.
- Craven, J.D., Frank, L.A. and Ackerson, K.L., *Geophys. Res. Lett.* Vol. 9, pp961, 1982.
- Evans, J.V., Holt, J.M., Oliver, W.L. and Wand, R.H., "The fossil theory of nighttime high latitude F-region troughs," *J. Geophys. Res.* Vol. 88. pp7769-7782, 1983.

Feinblum, D.A., "Hilion- A model of the high-latitude ionospheric F2-layer," *Tech. Rep. US Army Contr No DAHC 60-71-0005*. Bell Lab., Western Electric Whippany N.J. 07981.

Feinblum, D.A., Horan, R.J. and Hilion, "A model of the high latitude ionospheric F2-layer and statistics of regular ionospheric effects at Ft Churchill," 1968 report Bell Lab Murry Hill N.J. 1973.

Grebowsky, J.M., Hoffman, J.H. and Maynard, N.C., "Ionospheric and magnetospheric plasma-pauses," *Planet. Space Sci.* Vol. 26, pp651-660, 1978.

Grebowsky, J.M., Maynard, N.C., Tulunay, Y.K. and Lanzerotti, L.J., "Coincident observations of ionospheric troughs and the equatorial plasmasphere," *Planet. Space Sci.* Vol. 24, pp1177-1185, 1976.

Grebowsky, J.M., Taylor, H.A.Jr. and Lindsay, J.M., "Location and source of high latitude troughs," *Planet. Space Sci.*, Vol. 31, pp99-105, 1983.

Grebowsky, J.M., Tulunay, Y.K. and Chen, A.J., "Temporal variations in the dawn and dusk midlatitude trough and plasmopause position," *Planet. Space Sci.* Vol. 22, pp1089-1099, 1974.

Halcrow, B.W., "F2 peak electron densities in the main trough region of the ionosphere," *Report No PSU-IRL-IR-55 Contract NASA NGL 39-009-003* Ionospheric Research Lab., Pennsylv. State Uni. 1976.

Halcrow, B.W. and Nisbet, J.S., "A model of F2 peak electron densities in the main trough region of the ionosphere," *Radio Sci.*, Vol. 12, pp815-820, 1977.

Holt, J.M., and Evans, J.V., "Millstone Hill studies of the trough boundary between the plasmopause and magneto-Wand, R.H. sphere or not?" *Radio Sci.* Vol. 18, pp947-954, 1983.

Kavanagh, L.D., Freeman, S.W. and Chen, A.J., "Plasma flow in the magnetosphere," *J. Geophys. Res.* Vol. 73, pp5511-5519, 1968.

Knudsen, W.C., "Magnetospheric convection and the high latitudes F2 ionosphere," *J. Geophys. Res.*, Vol. 79, pp1046-1955, 1974.

Knudsen, W.C., Banks, P.M., Winningham, J.D., and Klumpar, D.M., "Numerical model of the convecting F2 ionosphere at high latitudes," *J. Geophys. Res.*, Vol. 82, pp4784-4792, 1977.

Kohnlein, W. and Raitt, W.J., "Position of the mid-latitude trough in the topside ionosphere as deduced from ESRO 4 observations," *Planet. Space Sci.*, Vol. 25, pp600-602, 1977.

Liszka, L., "The high-latitude trough in ionospheric electron content," *J.A.T.P.*, Vol. 29, pp1243-1259, 1967.

Liszka, L. and Turunen, T., "On the relation between auroral particle precipitation and the ionospheric trough," Kiruna Geophysical Observatory preprint No 70, 1970.

Mendillo, M. and Chacko, C.C., "The baseline ionospheric trough," *J. Geophys. Res.* Vol. 82, pp5129-5137, 1977.

Mendillo, M. and Klobuchar, J.A., "Investigations of the ionospheric F-region using multi-station total electron content observations," *J. Geophys. Res.* Vol. 80, pp643, 1975.

Moffet, R.J. and Quegan, S., "The mid-latitude trough in the electron concentration of the ionospheric F-layer. A review of observations and modelling," *J.A.T.P.* Vol. 45, pp315-343, 1983.

Morrell, C., "Sporadic-E (Es) associated with the main ionospheric trough observed over Halley station Antarctica," *Br. Antarct. Surv. Bull.* No 63, pp1-18, 1983.

Muldrew, D.B., "F-layer ionization troughs deduced from Alouette data," *J Geophys. Res.* Vol 70, pp2635-2650, 1965.

Murphy, J.A., Bailey, G.J. and Moffett, R.J., "Calculated daily variations of O^+ and H^+ at mid-latitudes. 1. Protonospheric replenishment and F-region behavior at sunspot minimum," *J.A.T.P.* Vol. 38, pp351-364, 1976.

Nagy, A.F., Robel, R.G. and Hays, P.B., *Space Sci. Rev.* Vol. 11, pp709, 1970.

Nichol, D.G., "Spread-F in mid-latitude trough zone," *J.A.T.P.* Vol. 35, pp1869, 1973.

Norton, R.B. and Findlay, J.A., "Electron density and temperature in the vicinity of the 29 September 1967 middle latitude red arc," *Planet. Space Sci.*, Vol. 17, pp1867, 1969.

Pinnock, M., "Observations of daytime mid-latitude ionospheric trough," *J.A.T.P.* Vol. 47, pp1111-1121, 1985.

Prolss, G.W. and Von Zahn, U., "ESRO 4 gas analyzer results 2. Direct measurements of changes in the neutral composition during an ionospheric storm," *J. Geophys. Res.* Vol. 79, pp2535-2539, 1974.

Quegan, S., Bailey, G.J., Moffet, R.J., Heelis, R.A., Fuller-Rowell, T.J., Rees, D. and Spiro, R.W., "A theoretical study of the distribution of ionization in the high-

latitude ionosphere and the plasmasphere; first results on the mid-latitude trough and the light-ion trough," *J.A.T.P.* Vol.44, pp619-640, 1982.

Raitt, W.J., Schunk, R.W. and Banks, P.M., "A comparison of the temperature and density structure in high and low speed thermal proton flows," *Planet. Space Sci.* Vol. 23, pp1103-1117, 1975.

Rodger, A.S., Brace, L.H., Hoegy, W.R. and Winningham, J.D., "The poleward edge of the mid-latitude trough, its formation, orientation and dynamics," *J.A.T.P.* Vol. 48, pp715-728, 1986.

Rodger, A.S., Morrell, C. and Deleney, J.R., "Studies of sporadic-E(Es) associated with the main ionospheric trough," *Radio Science* Vol. 18, pp937-946, 1983.

Rodger, A.S. and Pinnock, M., "The variability and predictability of the main ionospheric trough," Deehr, C.S and Holder, J.A. eds. *Exploration of the polar upper atmosphere.* (D. Reidel Publ. Co). pp463-469, 1980.

Rodger, A.S. and Pinnock, M., "Movements of the mid-latitude ionospheric trough," *J.A.T.P.* Vol. 44, pp985-992, 1982.

Rodger, A.S., Moffett, R.J. and Quegan, S., "The role of ion drift in the formation of ionization troughs in the mid- and high-latitude ionosphere - A review," *J.A.T.P.*, 54, pp. 1-30, 1992.

Rycroft, M.J., "A review of in situ observations of the plasmopause," *Annls. Geophys.* Vol. 31, pp1-16, 1975.

Rycroft, M.J. and Burnell, J., "Statistical analysis of movements of the ionospheric trough and the plasmopause," *J. Geophys. Res.*, Vol. 75, pp5600-5604, 1970.

Rycroft, M.J. and Thomas, J.O., "The magnetospheric plasmopause and the electron density trough at Alouette I orbit," *Planet. Space Sci.* Vol. 18, pp65-80, 1970.

Sharp, G.W., "Mid-latitude trough in the night ionosphere," *J. Geophys. Res.* Vol. 71, pp1345-1356, 1966.

Schunk, R.W., Banks, P.M. and Raitt, W.J., "Effects of electric fields and other processes upon the nighttime high-latitude F-layer," *J. Geophys. Res.* Vol. 81, pp3271-3282, 1976.

Schunk, R.W., Raitt, W.J. and Banks, P.M., "Effect of electric fields on the daytime high-latitude E and F regions," *J. Geophys. Res.* Vol. 80, pp3121-3130, 1975.

Sojka, J.J., Raitt, W.J. and Schunk, R.W., "A theoretical study of the high-latitude winter F-region at solar minimum for low magnetic activity," *J. Geophys. Res.*, Vol. 86, pp609-621, 1981a.

Sojka, J.J., Raitt, W.J. and Schunk, R.W., "Plasma density features associated with strong convection in the winter high-latitude F-region," *J. geophys. Res.*, Vol. 86, pp6968-6916, 1981b.

Sojka, J.J., Raitt, W.J., Schunk, R.W., Parish, J.L. and Rich, F.J., "Diurnal variation of the dayside, ionospheric mid-latitude trough in the southern hemisphere at 800 km: model and measurement comparison," *Planet. Space Sci.* Vol. 33 pp1375-1382, 1985.

Spiro, R.W., "A study of plasma flow in the mid-latitude ionization trough," *PhD dissertation University of Texas Dallas*, 1978.

Spiro, R.W., Heelis, R.A. and Hanson, W.B., "Ion convection and the formation of the mid-latitude F-region ionization trough," *J. Geophys. Res.* Vol. 83, pp4255-4264, 1978.

Spiro, R.W., Heelis, R.A. and Hanson, W.B., "Rapid subauroral ion drifts observed by Atmospheric Explorer C," *Geophys. Res. Lett.* Vol. 6, pp657-660, 1979.

Taylor, H.A.Jr., "The light ion trough," *Planet. Space Sci.* Vol. 20 pp1593-1605, 1972.

Taylor, H.A.Jr., Grebowsky, J.M. and Chen, A.J., "Ion composition irregularities and ionosphere-plasmasphere coupling: Observations of a high latitude ion trough," *J.A.T.P.* Vol. 37 pp613-623, 1975.

Taylor, H.A. and Walsh, W.J., "The light ion trough, the main trough and the plasmopause," *J. Geophys. Res.* Vol. 77, pp6716-6723, 1972.

Tulunay, Y.K., "Global electron density distributions from Ariel III satellite at mid-latitudes during quiet magnetic periods," *J.A.T.P.* Vol. 35, pp233-254, 1973.

Tulunay, Y.K. and Grebowsky, J.M., "The noon and midnight mid-latitude trough as seen by Ariel 4," *J.A.T.P.* Vol. 40, pp845-855, 1978.

Tulunay, Y.K. and Sayers, J., "Characteristics of the mid-latitude trough as determined by the electron density experiment on Ariel III," *J.A.T.P.* Vol. 33 pp1737-1761, 1971.

Wagner, R.A., Snyder, A.L. and Akasofu, S.I., *Planetary Space Science*, Vol.21, pp1911, 1973.

Watanabe, S., Oyama, K-I and Abe, T., "Electron temperature structure around mid-latitude ionospheric trough," *Planet. Space Sci.*, Vol. 37, pp1453-1460, 1989.

Whalen, J.A., "The daytime F layer trough observed on a macroscopic scale," *J. Geophys. Res.* Vol. 92, pp2571, 1987.

Whalen, J.A., "The daytime F-layer trough and its relation to ionospheric magnetospheric convection," *J. Geophys. Res.* 1989.

Wildman, P.J.L., Sagalyn, R.C. and Ahmed, M., "Structure and morphology of the main plasma trough in the topside ionosphere," Proceedings of the Cospar satellite beacon group on the geophysical use of satellite beacon observations. Michael Mendillo ed., 1-4 June 1976, Boston Uni. U.S.A.

Wrenn, G.L. and Raitt, W.J., "In situ observation of mid-latitude ionospheric phenomena associated with the plasmopause," *Ann. Geophys.*, Vol. 31, pp17-28, 1975.